uOttawa

L'Université canadienne
Canada's university

FACULTÉ DES ÉTUDES SUPÉRIEURES ET POSTOCTORALES

uOttawa

L'Université canadienne
Canada's university

FACULTY OF GRADUATE AND POSDOCTORAL STUDIES

Bo Yu

AUTEUR DE LA THÈSE / AUTHOR OF THESIS

M.A.Sc. (Chemical Engineering)

GRADE / DEGREE

Department of Chemical Engineering

FACULTÉ, ÉCOLE, DÉPARTEMENT / FACULTY, SCHOOL, DEPARTMENT

Sulfate Removal from Concentrated Sodium Chloride Brines for Chloralkali Industry with Nanofiltration Membranes

TITRE DE LA THÈSE / TITLE OF THESIS

Christopher Lan

DIRECTEUR (DIRECTRICE) DE LA THÈSE / THESIS SUPERVISOR

CO-DIRECTEUR (CO-DIRECTRICE) DE LA THÈSE / THESIS CO-SUPERVISOR

EXAMINATEURS (EXAMINATRICES) DE LA THÈSE / THESIS EXAMINERS

Arturo Macchi

Jason Zhang

Gary W. Slater

LE DOYEN DE LA FACULTÉ DES ÉTUDES SUPÉRIEURES ET POSTDOCTORALES /
DEAN OF THE FACULTY OF GRADUATE AND POSTDOCORAL STUDIES

Sulfate Removal from Concentrated Sodium Chloride Brines for Chloralkali Industry with Nanofiltration Membranes

by

Bo Yu

A thesis submitted to the Faculty of Graduate and Postdoctoral Studies

in partial fulfillment of the requirements for the degree of

MASTER OF APPLIED SCIENCE

in the Department of Chemical Engineering

University of Ottawa

Your file Votre référence
ISBN: 0-494-14976-0
Our file Notre référence
ISBN: 0-494-14976-0

Abstract

Nanofiltration membrane elements have been employed for the treatment of solutions containing raw brine generated by chloralkali industry. This study focused on the selection of appropriate nanofiltration membrane element and the assessment of their performance for the removal of sulfate and the retention of chloride from feed solutions. The influence of membrane type, temperature, pressure and sodium sulfate concentration on the selective removal of sulfate from concentrated sodium chloride brines were investigated. A high passage of sodium chloride and rejection of sodium sulfate were achieved with two different commercial nanofiltration membrane elements, DL2540 produced by GE Osmonics and NF270-2540 manufactured by FilmTec (Dow), suggesting that both membranes can be employed in sulfate removal from sodium chloride brines for chloralkali industry. Operating pressure and temperature showed no significant effects on sulfate rejection under the tested conditions. However permeate flux increased with both temperature and pressure in the tested ranges. The influence of temperature on permeate flux was due to the dependency of the viscosity of salt solution, which follows the Arrhenius model. Sodium concentration in feed had significant effects on permeate flux, sulfate rejection, and sulfate concentration at membrane interface and in permeate. Sulfate rejection and permeate flux reduced sharply with the increase of sulfate concentration in feed.

Résumé

Les éléments de membrane de Nanofiltration ont été employés pour le traitement de solutions contenant la saumure brute produite par l'industrie chloralcali. Cette étude s'est concentrée sur le choix d'élément approprié de membrane de nanofiltration et de l'évaluation de leur performance pour l'enlèvement de sulfate et de la rétention de chlorure des solutions de nourriture. L'influence du type de membrane, la température, pression et la concentration en sulfate de sodium sur le déplacement sélectif de sulfate des saumures de chlorure de sodium concentrées ont été enquêtées. Une passage élevée du chlorure de sodium et le rejet du sulfate de sodium ont été réalisés avec deux éléments commerciaux de membrane de nanofiltration, DL2540 produit par GE Osmonics et NF270-2540 fabriqué par FilmTec (Dow), en suggérant que les deux membranes peuvent être employées dans l'enlèvement de sulfate des saumures de chlorure de sodium pour l'industrie chloralcali. La pression de fonctionnement et la température n'ont montré aucun effet significatif sur le rejet de sulfate dans les conditions évaluées. Cependant, le flux perméable a augmenté avec la température et la pression dans les gammes examinées. L'influence de la température sur le flux perméable était due à la dépendance de la viscosité de la solution de sel, qui suit le modèle d'Arrhenius. La concentration de sodium dans l'alimentation a eu des effets significatifs sur le flux, le rejet de sulfate, et la concentration perméable en sulfate à l'interface de membrane et dans l'imprégnation. Le rejet de sulfate et le flux perméable ont réduit brusquement avec l'augmentation de concentration de sulfate dans l'alimentation.

Acknowledgements

I wish to express my sincere thanks to my supervisor Dr. C. Lan and co-supervisor Dr. A. Tremblay for their supervision and guidance throughout this research work. I also wish to thank Dr. Z. Duvnjak for his support.

I would like to thank Louis Tremblay, Gerard Nina and Franco Ziroldo for their assistance in the lab. I also wish to thank the Department's administrative and support staff for their help.

Finally, I wish to thank my wife, Yue Ma, and our son YuanQing Yu, for their love, support, encouragement and understanding throughout my studies at the University of Ottawa.

Nomenclature

A	chloride ion activity
a	activity, mol m^{-3}
a_i	activity of ion i, mol m^{-3}
C_1	concentration in bulk solution, mol/m^3
C_2	concentration on membrane sulface, mol/m^3
C_3	concentration in permeate, mol/m^3
C_i^0	bulk concentration of ion i. mol/m^3
c_i	concentration of component i in membrane, mol/m^3
$C_{i,m}$	concentration of ion i at the membrane interfaces of feed side, mol/m^3
$C_{i,p}$	concentration of ion i at the membrane interfaces of permeate side, mol/m^3
$C_{i,b}$	concentration of component i in bulk solution, mol/m^3
$C_{i,p}$	concentration of component i in permeate, mol/m^3
$D_{i,p}$	hindered diffusivity, m^2s^{-1}
$D_{i,\infty}$	bulk diffusivity, m^2s^{-1}
E	measured electrode potential, V
E^0	constant, the sum of several system potentials, V
E_p	the apparent activation energy for permeation, J
F	Faraday constant, C mol^{-1}
G	the hydrodynamic lag coefficient
j_i	ion flux (based on membrane area), mol m^2 s^{-1}
J_v	volume flux (based on membrane area), ms^{-1}
K^1	the hydrodynamic enhanced drag coefficient

$K_{i,c}$	hindrance factor for convection
$K_{i,d}$	hindrance factor for diffusion
L	length of the membrane module, m
L_P	membrane permeability (L/h-m^2-PSI)
M_w	molecular weight, g mol^{-1}
P	passage of solute or pressure, N m^2
Pe_m	Peclet number
P_m	water permeability, m s^{-1} Pa^{-1}
ΔP	applied pressure drop, kN m^{-2}
r_p	effective pore radius, m
r_s	stock redius of ions and solutes, m
R	rejection of solute or gas constant, J mol^{-1} K^{-1}
S	electrode slope
T	absolute temperature, K
V	solute velocity, m s^{-1}
V_i	partial molar volume of ion i, m^3 mol^{-1}
X	the effective volumetric membrane charge density.
X_D	effective membrane charge, mol m^{-3}
x	distance normal to membrane, m
Δx	effective membrane to thickness, m
z_i	valence of ion i, dimensionless

Φ	steric partition term
λ	ratio of ionic or solute radius/pore radius
μ	viscosity of solution, Pa s
μ_i	the electrochemical potential, V
ξ	ratio of effective charge density to bulk concentration
π	osmotic pressure, kN m^{-2}
γ_i	activity coefficient of ion *i* with membrane
γ^0_i	bulk activity coefficient of ion *i*
γ_k	activity coefficient
ψ	potential within the pore, V
ψ_m	electric potential in axial direction inside membrane, V
$\Delta\psi_m$	potential difference inside membrane
$\Delta\psi_D$	Donnan potential difference, V

Table of Contents

List of Tables

List of Figures

1. Introduction

1.1 Project background

Chloralkali industry is a key contributor to the economic, social and environmental well-being of society. In the chlorine making process, high concentration of sodium chloride (NaCl) brine is electrolyzed to produce gaseous chlorine (Cl_2), hydrogen (H_2) and sodium hydroxide (NaOH), see Figure 1-1.

A typical chloralkali plant consists of six main process areas:

1. Brine preparation
2. Electrolysis
3. Chlorine handling
4. Caustic handling
5. Hydrogen handling
6. Hypochlorite

Chlorine and sodium hydroxide are produced from the electrolysis of an aqueous solution of sodium chloride brine. Hydrogen gas is produced as a byproduct of the chloralkali process. The chemical equation for the overall reaction taking place in an electrolysis cell is illustrated in the following equation:

$$2\ NaCl\ (aq) + 2\ H_2O\ (l) + \text{electric current} \rightarrow H_2\ (g) + Cl_2\ (g) + 2\ NaOH\ (aq) \qquad (1\text{-}1)$$

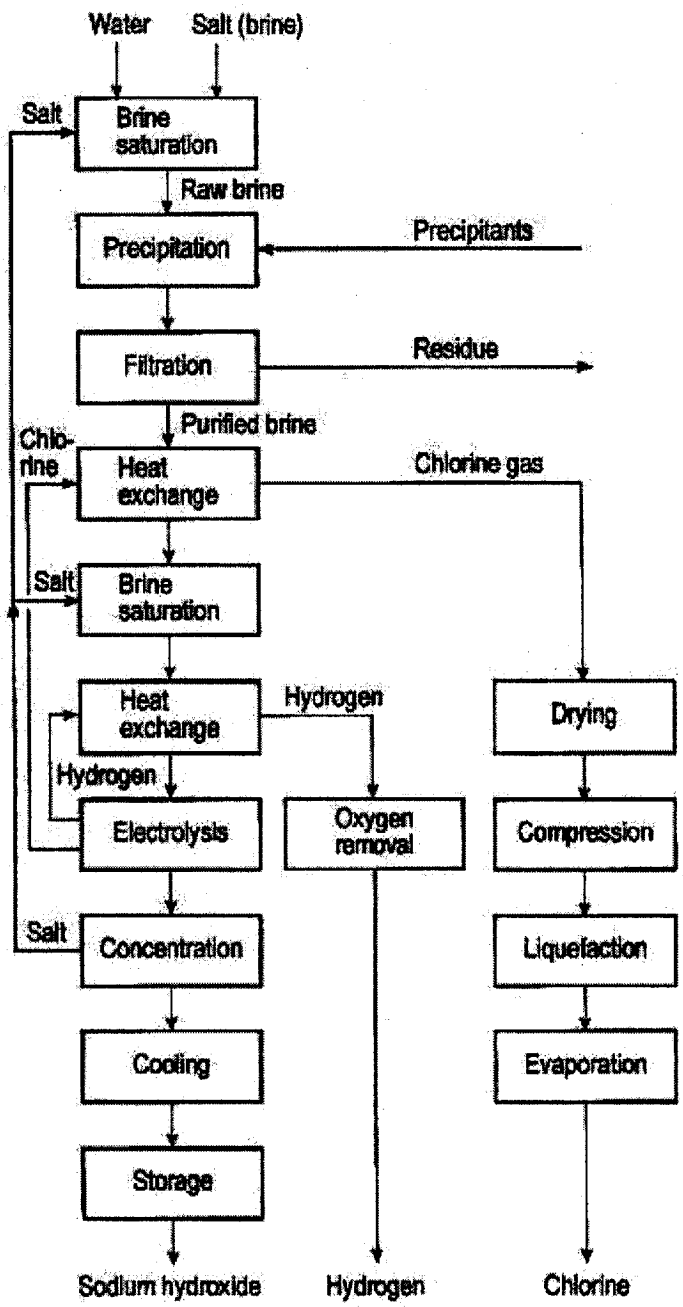

Figure 1-1 Chloralkali industry process

For a close up view of what an electrolysis cell may resemble, see Figure 1-2 blow.

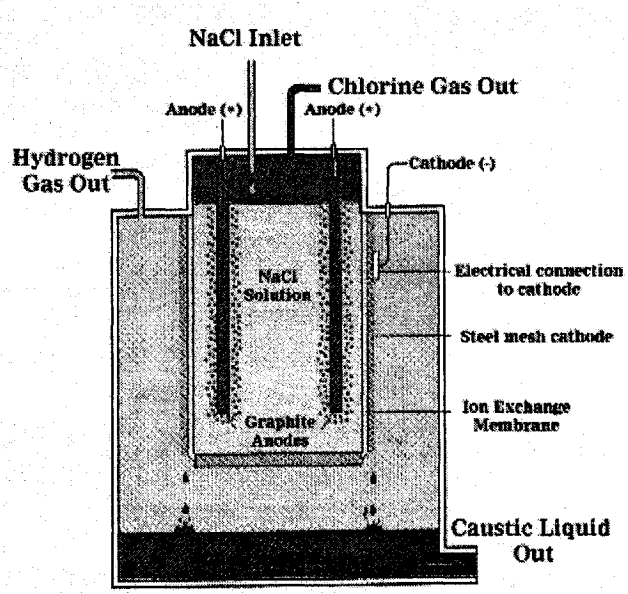

Figure 1-2 Electrolysis cell

Industrial salt (NaCl) always contains a small amount of sulfate, which is not subject to any change in the electrolysis process and will accumulate if not removed from the recycled brine. The accumulation of sulfate in brine may cause precipitation on the electrode surface in the electrolysis cell, which leads to high voltage requirement and power consumption. Most importantly, the precipitation may significantly reduce the lifetimes of the expensive electrodes and the ion exchange membrane used in the electrolysis cell. Therefore, selective removal of sulfate from concentrated brine is needed for the chloralkali industry to address this concern.

Conventional methods of sulfate removal are either the purging of brine to the sewer or nearby water body or by reaction with barium chloride to form solid barium sulfate for downstream removal by filtration [1].

The purging method of sulfate removal results in an effluent brine stream that for some plants contains mercury (which is toxic and strictly regulated). This brine purge is the largest component of total effluent from a typical chloralkali plan and results in a significant discharge to the environment. In addition, the brine purge stream results in lost economic value to the plan operators since costs are incurred for the supply and purification of the salt that is lost.

The barium method of sulfate removal involves the reaction of sulfate in the brine with added barium chloride to form an insoluble barium sulfate precipitate that is filtered out and disposed to landfill. Problems with this method include the cost and handling of toxic barium chloride and the production of solid waste for disposal.

The nanofiltration (NF) membrane can separate the sulfate ions from the salt ions in a brine solution at a molecular level and has recently gained high interest and acceptance by the chloralkali industry. Sulfate removal for chloralkali brine is expected to increase worldwide. This technology will serve to expand in reducing waste stream volume and contributing to sustainability around world.

In real industrial application, the membrane assembly unit consists of a stand supporting the pressure vessels, interconnecting piping, and feed, permeate and concentrate manifolds. spiral-wound membrane elements are installed in the pressure

vessels. Figure 1-3 shows a spiral element with spacer and membrane leafs in their unwound state. The concentrate spacer keeps the two membrane sides of the high pressure envelope at a distance of 0.5 to 1.0 mm. The concentrate (also called retentate) follows nearly straight macroscopic streamlines parallel to the axis of the module. The permeate spirals inwardly through the permeate envelope to the central collection pipe. The flow modes of concentrate and permeate correspond to cross-flow.

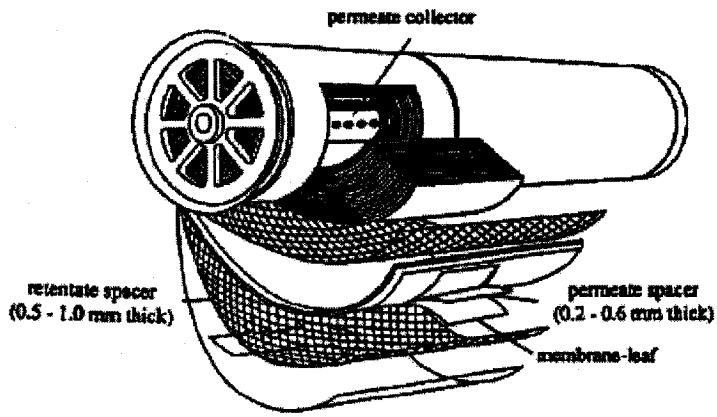

Figure 1-3 Structural elements of a spiral-wound membrane element (in its partly unwound state)

The pressure vessel has permeate ports on each end, located in center of the end plate, and feed and concentrate ports, located on the opposite ends of the vessel. Each pressure vessel may contain from one to seven membrane elements connected in series.

As shown in Figure 1-4, the permeate tube of the first and the last element is connected to the end plates of the pressure vessel. Permeate tubes of elements in the pressure vessel are connected to each other using interconnectors. On one side of each membrane element there is a brine seal, which closes the passage between outside rim of the element and inside wall of the pressure vessel. This seal prevents feed water from bypassing the membrane module, and forces it to flow through the feed channels of the element [2].

As feed water flows through each subsequent membrane element, part of the feed volume is removed as permeate. The salt concentration of the remaining feed water increases along the pressure vessel. Permeate tubes conduct the permeate from all connected elements. The collected permeate has the lowest salinity at the feed end of the pressure vessel, and increases gradually in the direction of the concentrate flow.

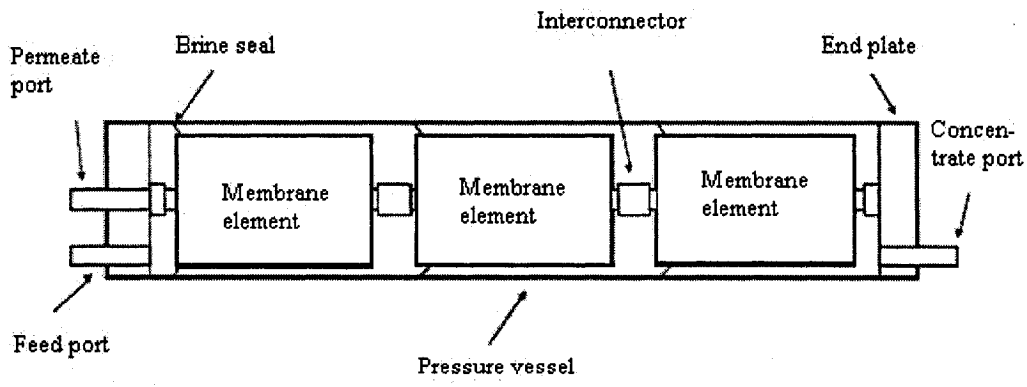

Pressure vessel with three membrane elements

Figure 1-4 Membrane element configuration

A system is divided into groups of pressure vessels, called concentrate stages. In each stage pressure vessels are connected in parallel, with respect to the direction of the feed/concentrate flow. The number of pressure vessels in each subsequent stage decreases in the direction of the feed flow, usually in the ratio of 2:1, as shown in Figure 1-5 [2].

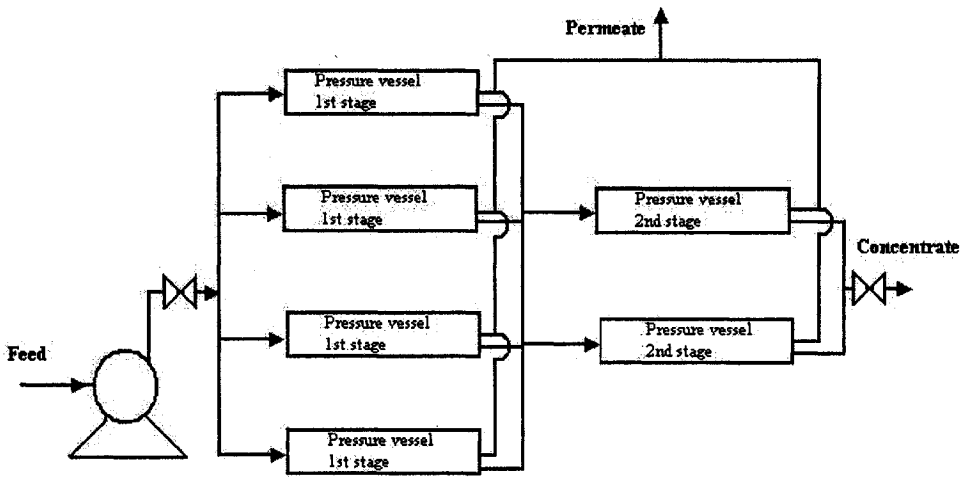

Figure 1-5 Flow diagram of a two stage system

Thus, one can visualize that the flow of feed water through the pressure vessels of a system resembles a pyramid structure: a high volume of feed water flows in at the base of pyramid, and a relatively small volume of concentrate leaves at the top. The decreasing number of parallel pressure vessels from stage to stage compensates for

the decreasing volume of feed flow, which is continuously being partially converted to permeate. The permeate of all pressure vessels in each stage, is combined together into a common permeate manifold. So the volume of final retention will be significantly reduced and the rejected solute (sodium sulfate) will be concentrated.

1.2 Purpose of the study

The objective of this project is to investigate the influence of operating conditions on the commercial nanofiltration membrane elements. This study focused on the selection of membranes and operating conditions to obtain a maximum rejection rate of sulfate and passage rate of chloride as well as high permeate flux. The results will provide useful guidelines for industrial design of sulfate removal for chloralkali industry.

1.3 Perspectives of NF membrane process

In a membrane separation process, the feed is a mixture of phases. The membrane is preferentially selective to one or more of the species in the feed mixture. The result will be two new phases, one is enriched with the selected species and the other is depleted. The enriched phase is called retentate or concentrate stream and the depleted phase is called the permeate stream (Figure 1-4), which implies that either the concentrate or the permeate stream is the product. If the aim is concentration, the retentate will usually be the product stream. However, in the case of purification, both the retentate or permeate can yield the desired product.

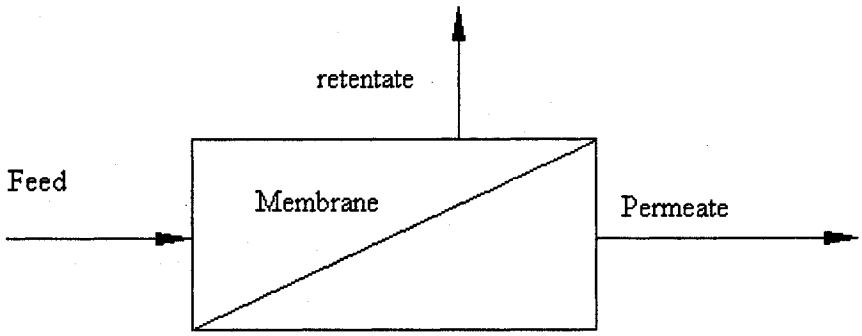

Figure 1-6 Schematic representation of a membrane process

Beginning in the late 60s, gradually membrane processes have found their way into industrial application and serve as alternatives for many traditional processes such as distillation, evaporation and extraction. Based on the main driving force of membrane separation process, the membrane processes can be categorized as given in Table 1-1.

Table 1-1 Driving forces and their related membrane separation processes

Driving force	Membrane process
• Pressure difference	Microfiltration, ultrafiltration, nanofiltration, reverse osmosis
• Chemical potiential difference	Pervaporation, pertraction, dialysis, gas separation, vapor permeation, liquid membranes
• Electrical potiential difference	Electrodialysis, membrane electrophoresis, membrane electrolysis
• Temperature difference	Membrane distillation

Nanofiltration (NF) membrane is a pressure driven membrane process and represents a specific domain of membrane technology that is a relatively new. It has properties in between ultrafiltration (UF) membranes and reverse-osmosis (RO) membranes. NF membranes, with average pore radius in the nanometer range, have separation properties in between those of RO and UF membranes. They also have a special feature, the high retention of charged particles (ions), due to the fact that NF membranes carry charges in an aqueous environment. Figure 1-7 illustrates the filtration spectrum of membrane.

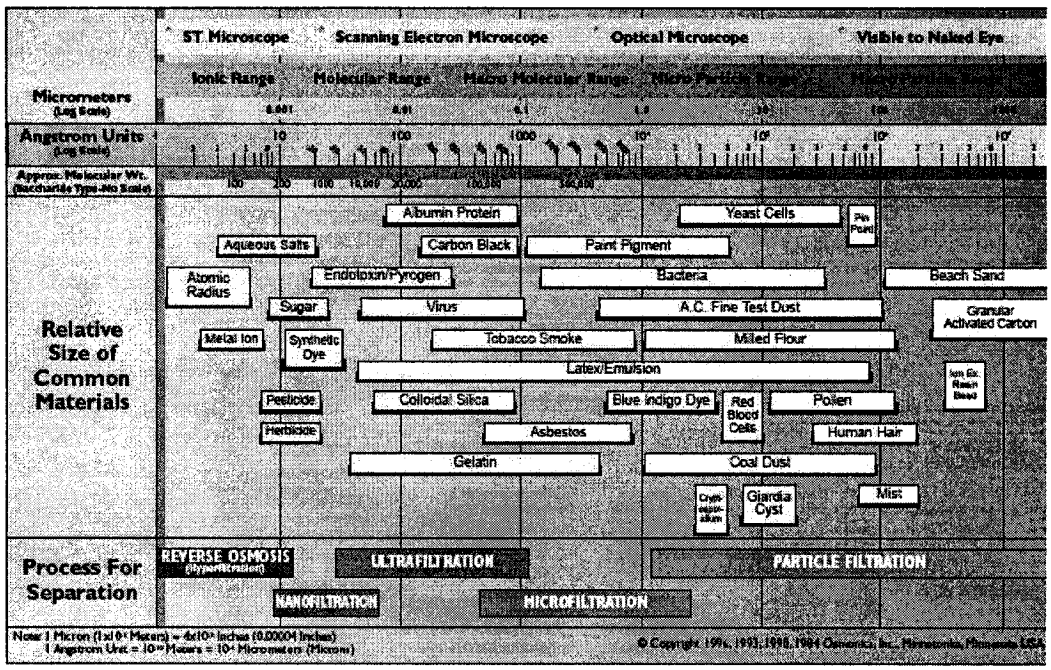

Figure 1-7 Filtration spectrum of membrane

Generally, NF membrane has two distinct properties [3]:

- The pore size of the membrane corresponds to a molecular weight cut off value of approximately 150-1500 $\frac{g}{mol}$. Therefore, the separation of

components with these molecular weights from higher molecular weight components can be accomplished.

- NF membranes have a slightly charged surface. Because the dimensions of the pores are less than one order of magnitude larger than the size of ions, charge interaction plays a dominant role. This effect can be used to separate ions with different valences.

Rejection of charged solutes by NF membranes is a rather complicated phenomenon and has yet to be completely understood. Various mechanisms are involved in the process such as electrostatic interactions between the membrane and the charged species, sieving or size effect, differences in diffusivity and solubility, dielectric repulsions, etc.

NF membranes also show selectivity based on charge density of the ion. For ion-selective membranes with solutions containing different free ions, an unequal distribution of ions results across the membrane, and forms a high concentration thin boundary layer on membrane surface of feed side. This is known as the Donnan effect. Based on the literature review [3, 4], when Na_2SO_4 is added to a solution of constant NaCl concentration, Cl^- ions are forced to permeate preferentially compared to SO_4^{2-} ions together with Na^+ ions in order to maintain electroneutrality at both sides of the membrane: the Cl^- rejection decreases with increasing of Na_2SO_4 concentration and even negative rejection coefficients can be observed.

Since most NF membranes contain negatively charged hydrophilic groups attached to a hydrophobic UF support membrane, they have higher water fluxes than do RO

membranes. This is due to the favorable orientation of water dipoles. They also have improved fouling resistance against hydrophobic colloid. This makes NF competitive with RO in high-fouling applications such as dye concentration and power-waste treatment. However, for solutes with a charge opposite to the membrane charges may increase fouling. NF membranes are best in applications that reject uncharged molecules due to size exclusion and charged components due to electrostatic interaction.

1.4 Industrial applications of NF membranes

The advantage of NF membrane process is low operating pressures compared with RO, and high rejection of organics compared with UF. NF is generally used to separate multivalent ions and organic components with relatively low molecular weight (150-1500 $\frac{g}{mol}$) from water.

Presently NF membrane has already gained its wide application in various industries areas, such as food, textile, clothing and leather, paper and graphical, chemical, water production etc. An overview of the possible applications of NF membrane is given in Table 1-2, which shows the diversity of opportunities for NF membrane. It can be expected that many are to follow or already exist. All applications are in the treatment of aqueous systems.

Table 1-2 Industrial applications of NF membrane

Industry	Application
Food	Demineralization of whey [5-7]
	Demineralization of sugar solutions [8]
	Recycle of nutrients in fermentation processes [9]
	Separation of sunflower oil from solvent [10]
	Recovery of Cleaning-In-Place solutions [11]
	Recovery of regeneration liquid from decolouring resins in sugar industry [12-15]
	Effluent treatment [16]
	Purification of organic acids [17-19]
Textile	Separation of amino acids [20]
	Removal of dyes from waste water [21]
Clothing and leather	Recovery of water and salts from waste water [22-24]
Paper and graphical	Recovery and reuse of chromium(III) and chromium(II) [25, 26]
	Recovery of water from waste water or waste water treatment effluent [27-29]
Chemical	Recovery of bleaching solution [30, 31]
	Sulfate removal preceding chlorine and NaOH production [32-34]
	CO_2 - removal from process gasses [35]
	Preparation of bromide [36]
	Recovery of caustic solutions in cellulose and viscose production [37]
	$CaSO_4$ precipitation [38]
Metal plating and	Separation of heavy metals from acid solutions [39, 40]
product/electronic	Removal of metal sulfates from waste water [41]
and optical	Cleaning of machine rinsing solutions [42]
	Removal of Nickel [43]
	Recovery of Cu-ions from ore extraction liquids [44-46]
	Al^{3+} removal from canning industry waste water [47]
Water production	Recovery of LiOH during treatment of battery waste [48]
	Removal of degreasing agents from water [49-52]
	Removal of precursors of disinfection byproducts [53]
	Hardness removal [54, 55]
	Removal of natural organic matter (a.o. colour) [56-59]
	Removal of pesticides [60-62]
	Removal of heavy metals (As, Pb), Fe, Cu, Zn and silica [63, 64]
Landfills	Removal of phosphate, sulfate, nitrate and fluoride [65-67]
Agriculture	Removal of algal toxins [68, 69]
	Purification of landfill leachate [70-76]
	Removal of selenium from drainage water [77]

2 Theoretical background

2.1 Mass transfer in nanofiltration membrane

A representation of the mass transfer process taking place in NF membrane can be given in Figure 2-1

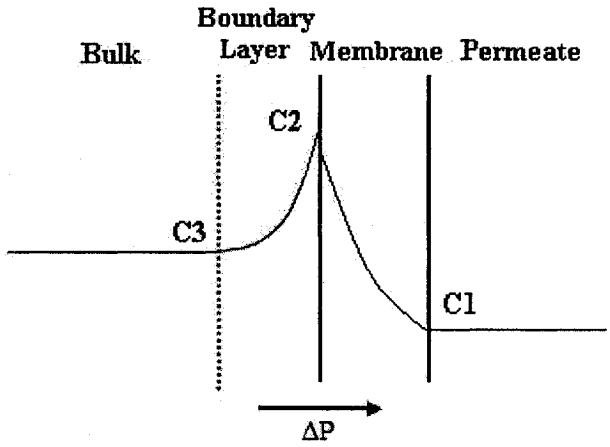

Figure 2-1 Mass transfer in NF membrane

When an external pressure ΔP is imposed on a liquid which is adjacent to a semi-permeable membrane, solvent will flow through the membrane. The general terms that are used in the description of membrane separation processes are the permeate flux (J) and the rejection (R). The permeate flux is given by [78, 80]:

$$J = \frac{Q_P}{A} = \frac{\Delta P - \pi}{\mu(R_m + R_f)} \qquad (2\text{-}1)$$

where Q_P is the volumetric flowrate of permeate and A the active membrane area. ΔP is the pressure drop and π is the osmotic pressure across the membrane (N/m^2), μ is the permeate viscosity (Pa.s), R_m is the initial membrane resistance and R_f is the resistance of a fouling layer (m^{-1}), π represents osmotic pressure.

Osmotic pressure appears to have first been described in 1748 by the Abbe Nollet [81]. The studies of van't Hoff in 1885 established a relationship between osmotic pressure, π, and concentration for dilute solutions,

$$\pi = cRT \tag{2-2}$$

where c is the concentration in *mol/l*. However, for high concentration solution such as our case, the above equation is not applicable. From thermodynamic considerations [81, 82], the osmotic pressure π for high concentration solution can be calculated by [82, 83]:

$$\pi = -k_p T \ln(1 - f) \tag{2-3}$$

where $k_p = \frac{R}{V} = 4.555\ (\frac{atm}{K})$, R is gas constant = 0.082 05 $(\frac{L \cdot atm}{K \cdot mol})$, V the molar volume of water, which is 0.018015 (L), and π is expressed in atmospheres.

In equation (2-3), f is the mole fraction of solute particles or sum of ions. When there are more than one solutes, this term should be express as Σf. The relevant quantity in this relation is $(1 - \Sigma f)$, which represents the mole fraction of water.

$$\pi = -k_p T \ln(1 - \sum_i f_i) \qquad (2\text{-}4)$$

A neutral solute dissolved in the solvent at a concentration level C_3 will also flow towards the membrane. If the membrane exhibits rejection for the solute, partial permeation will occur and non-permeated solute accumulates in the boundary layer, and hence a concentration profile develops. This phenomenon is called concentration polarization [84, 85]. The solute distributes at the membrane/solution interface and will be transported through the membrane by convection and diffusion. At the permeate side, a second distribution process will occur and a final concentration of solute in the permeate, C_1, will be reached. For the characterization of solute behavior, the rejection (R), passage (P) and selective (S) are used, given by (see Figure 2-1):

$$R = 1 - \frac{C_1}{C_3} \qquad (2\text{-}5)$$

$$P = \frac{C_1}{C_3} \qquad (2\text{-}6)$$

$$S = \frac{P}{1 - R} \qquad (2\text{-}7)$$

At steady state, the rate of solute arriving at the membrane is balanced by the sum of the solute leakage and the rate of back diffusion [78]:

2.2 Transport Model for nanofiltration Membranes

A transport model is needed in order to evaluate the value of the effective charge density as described previously and also to analyze the contribution of each of the transport mechanisms. Numerous papers have been published devoted to models that are likely to provide a description of the separation properties of NF membranes. Many theories treating the separation of multicomponent electrolytic system are based on extended Nernst-Planck equation, which is the basis for description of solute transport through nanofiltration membranes. In the extended Nernst-Planck equation, the ionic flux of component *i* is defined as follows

$$j_i = -\frac{c_i D_{i,p}}{RT} \cdot \frac{d\mu_i}{dx} + K_{i,c} c_i V \qquad (2\text{-}8)$$

where μ_i is the electrochemical potential defined as follows:

$$\mu_i = RT \ln a_i + V_i P + z_i F \psi + cons\tan t \qquad (2\text{-}9)$$

where a_i is the activity of ion *i*, mol m^{-3}; V_i partial molar volume of ion *i*, m^3 mol^{-1}; F Faraday constant, C mol^{-1}; P pressure, N m^2; z_i valence of ion *i*; ψ potential within the pore, V

The standard approach used to relate ion activity to its concentration is through an activity coefficient ($a_i = \gamma_i c_i$). Differentiation of equation (2-9) and substitution into equation (2-8) and manipulation yield the following transport equation:

$$j_i = -c_i D_{i,p} \frac{d[\ln \gamma_i]}{dx} - \frac{c_i D_{i,p}}{RT} V_i \frac{dP}{dx} - D_{i,p} \frac{dc_i}{dx} - \frac{z_i c_i D_{i,p}}{RT} F \frac{d\psi_m}{dx} + K_{i,c} c_i V$$

(2-10)

The first two terms in this expression are in addition to the three transport terms included in the most commonly used NF models. It should also be noted that, in the present case, ion flux is defined on a pore area basis. It will be assumed that the gradient of ln γ_i can be neglected, which implies that either the concentrations within the pore are small or their variations are small. So the extended Nernst-Planck equation can be developed to DSPM (Donnan-Steric partitioning Pore Model) (Eq. 2-11) [85, 86, 87].

DSPM model has been applied to analyze retention properties of a variety of nanofiltration membranes. Within the scope of this model, the solute transfer is described as being the result of the following steps: first, a distribution of charged species at the membrane–solution interface resulting from both size effects and Donnan exclusion and second, a transfer by a combination of convection, diffusion and electromigration through the membrane.

$$j_i = -D_{i,p} \frac{dc_i}{dx} - \frac{z_i c_i D_{i,p}}{RT} F \frac{d\psi_m}{dx} + K_{i,c} c_i V \qquad (2\text{-}11)$$

Where $D_{i,p} = K_{i,d} D_{i,\infty}$

j_i is the flux of ion i and the terms on the right hand side represent transport due to diffusion, electric field gradient and convection respectively (see List of symbols for

definition of symbols). The hindered nature of diffusion and convection of the ions inside the membrane are accounted for by the terms $K_{i,d}$ and $K_{i,c}$.

The hindrance factors, $K_{i,d}$ and $K_{i,c}$, which are functions of the ratio of solute to pore radius (λ), are related to the hydrodynamic coefficients K^{-1}, the enhanced drag, and G, the lag coefficient, of a spherical solute moving inside a cylindrical pore of infinite length. Bowen [85] reviewed the various equations that were used to calculate K^{-1} and G by finite-element technique and centre-line approach for λ ranging from 0 to 0.8, and gave his equations to calculate K^{-1} and G as flowing:

$$K^{-1}(\lambda,0) = 1.0 - 2.30\lambda + 1.154\lambda^2 + 0.244\lambda^3 \qquad (2\text{-}12)$$

$$G(\lambda,0) = 1.0 + 0.054\lambda - 0.988\lambda^2 + 0.441\lambda^3 \qquad (2\text{-}13)$$

For NF membranes the pore radii are very small and thus, the solute velocity might not be fully developed. If one were to assume a homogenous velocity for transport across the membrane, $K_{i,d}$ and $K_{i,c}$ are related to the hydrodynamics coefficients as [86],

$$K_{i,d} = K^{-1}(\lambda,0)$$

$$K_{i,c} = G(\lambda,0) \qquad (2\text{-}14)$$

If, however, the solute velocity is fully developed inside the pore and has the parabolic profile of the Hagen-Poiseuille type, the hindrance factors become [86],

$$K_{i,d} = K^{-1}(\lambda,0)$$

$$K_{i,c} = (2-\Phi)(\lambda,0) \qquad (2\text{-}15)$$

where

$$\Phi = (1-\lambda)^2 \qquad (2\text{-}16)$$

The steric term, Φ, accounting for the finite size of the solute, is referred as the homogenous membrane type and the latter as the porous membrane type.

For charged solutes, Eq. (2-11) is the basic equation for the transport of ions inside the membrane. The variation of equation (2-11) is due to the velocity distribution, as has been mentioned above, which leads to different definitions of the hindrance factors. For porous membranes, the fluxes, concentrations, potentials, and velocity were all defined in term of radial averaged quantities (DSPM). For homogenous membranes, the quantities do not have any radial distribution and are constant at any plane in the x-direction.

The conditions of electroneutrality in the bulk solution and inside the membranes are expressed respectively as:

$$\sum_{i=1}^{n} z_i C_i^0 = 0$$

$$\sum_{i=1}^{n} z_i c_i = -X_d \qquad (2\text{-}17)$$

where C_i^0 is the bulk concentration of ion *i*. c_i the concentration of ion *i* inside the membrane. and X_d the effective volumetric membrane charge density. X_d assumed to be constant at all points in the active part of the membrane. The zero current condition inside the membrane can be expressed as:

$$I_c = \sum_{i=1}^{n} F(z_i j_i) = 0 \tag{2-18}$$

Since the electric potential gradient is common for every ion inside the membrane, the electric potential and concentration gradients can be derived from equation (2-11). By rearranging equation (2-11), the concentration gradients is written as,

$$\frac{dc_i}{dx} = \frac{J_V}{D_{i,p}}(K_{i,c}c_i - C_{i,p}) - \frac{z_i c_i}{RT} F \frac{d\psi}{dx} \tag{2-19}$$

where the flux of ion j_i is expressed as,

$$j_i = J_V C_{i,p} \tag{2-20}$$

Use the same way, by rearranging equation (2-11), the potential gradient term can be written as,

$$\frac{d\psi}{dx} = \frac{\sum_{i=1}^{n}(K_{i,c}c_i - D_{i,p}\frac{dc_i}{dx} - j_i)}{\frac{FD_{i,p}}{RT}\sum_{i=1}^{n} z_i c_i}$$

$$\frac{d\psi}{dx} = \frac{\sum_{i=1}^{n}(K_{i,c}c_i j_V z_i - j_V C_{i,p}) - D_{i,p}\frac{\sum_{i=1}^{n} dz_i c_i}{dx}}{\frac{FD_{i,p}}{RT}\sum_{i=1}^{n} z_i^2 c_i}$$

$$\frac{d\psi}{dx} = \frac{\sum_{i=1}^{n}\frac{z_i j_V}{D_{i,p}}(K_{i,c}c_i - C_{i,p})}{\frac{F}{RT}\sum_{i=1}^{n} z_i^2 c_i} \qquad (2\text{-}21)$$

By using the following boundary conditions together with the equation for electroneutrality (13):

$X = 0$ $\qquad C_i = C_{i,m}$

$X = \Delta x$ $\qquad C_i = C_{i,p}$

where $C_{i,m}$ and $C_{i,p}$ are concentration of ion i at the membrane interfaces of feed side and permeate side respectively. The concentration at the interface can be determined using the following equilibrium conditions which will be taken as a combination of the Donnan and steric effects:

$$\frac{\gamma_i c_i}{\gamma_i^0 c_i^0} = \Phi \exp(-\frac{z_i F}{RT}\Delta\Psi_D) \qquad (2\text{-}22)$$

where γ_i is activity coefficient of ion *i* with membrane; γ^0_i bulk activity coefficient of ion *i*; ψ_D Donnan potential, N m^{-2}. The term Φ is the steric partitioning term to account for the steric effects on the entrance to the membrane and is given by Eq. (2-11)

3 Experiment methodology

3.1 Preparation of synthetic sodium chloride brine

Synthetic sodium chloride brines were made up from crystalline sodium chloride (Certified ACS), powder sodium sulfate anhydrous (USP/FCC) and distilled water. By dissolving appropriate amounts of sodium chloride and sodium sulfate into distilled water, the concentrations of sodium chloride and sodium sulfate are 200 g/L and 10.0 g/L, respectively. This formed the basis for the makeup of standard synthetic sodium chloride brine used as feed solutions in all constant feed concentration tests. Sodium chloride and sodium sulfate were purchased from Fisher Scientific Canada with category number of S271-50 and S429-12 respectively.

3.2 NF membranes

Based on the information, which showed high rejection to sulfate and passage to chloride, collected from manufactures, three types of NF membrane elements were employed for test. These were: NF270-2540 from FilmTec (DOW), DL2540F from GE Osmonics Inc., and XN45-2540 from TriSep Co.

All the membranes are made of polyamide material, DL2540F and NF270-2540 membranes have molecular weight cutoffs between 150 to 300 Dalton., the XN45-2540 membrane has molecular weight cutoff range of 500-1000 Dalton The technical specifications provided by manufacturers are summarized in Table 3-1.

Table 3-1 Characteristics of the NF membrane elements used in tests

Manufacturer	GE Osmonics	FilmTec (DOW)	TriSep
Membrane element	DL2540F	NF270-2540	XN45-2540
Membrane Type	Proprietary Thin-Film Composite	Polyamide Thin-Film Composite	XN45TM Polyamide-Urea NF membrane
Cut-Off Range	150-300 Da	200-300	500-1000
Maximum Operating Temp.	122°F (50 °C)	113°F (45 °C)	113°F (45 °C)
Maximum Operating Pressure	500 PSIG	600 PSIG (41bar)	600 PSIG
pH Range, cont. Operation	2-11	3-10	3-11
pH Range, short-term Cleaning (30 min)	1-11.5	1-12	NS[1]
Maximum Feed SDI	NS	5	5
Free Chlorine Tolerance	1000 ppm-hour	<0.1 ppm	<1.0 ppm
Stabilized $CaCl_2$ rejection	NS	40-60%[2]	NS
Stabilized $MgSO_4$ rejection	96%[3]	>97%[4]	>92%[3]
Active Area	3.2 m^2	3.2 m^2	3.2 m^2

[1] NS - not specified

[2] Based on a 500 mg/L $CaCl_2$ solution, 70 PSI, 25°C, and 15% recovery

[3] Based on a 2,000 mg/L $MgSO_4$ solution at 100 PSI net pressure, 25°C, 10% recovery, after 24 hours

[4] Based on a 2,000 mg/L $MgSO_4$ solution at 70 PSI net pressure, 25°C, 10% recovery, after 24 hours

3.3 Experimental set-up

All tests were performed using the pilot scale experimental set-up shown in Figure 3-1 and 3-2. In this system, a 250 liter feed tank provided feed solution to a 5 horsepower (HP) 16-stage centrifugal pump (ITT-G&L Pumps, SSV series, USA). A cooling coil was placed inside the feed tank in order to control the temperature of the solution. A stainless steel membrane housing, which a 40.5 inches long and 2.5 inches diameter nanofiltration membrane element was placed inside, was operated in crossflow. Permeate was circulated back to the feed tank. When performing volume reduction test, permeate was collected to a separately tank. Retentate and bypass stream were also returned back to the feed tank. This system was operated in a batch mode with maximum feed volume of 200 L and minimum volume of 30 L.

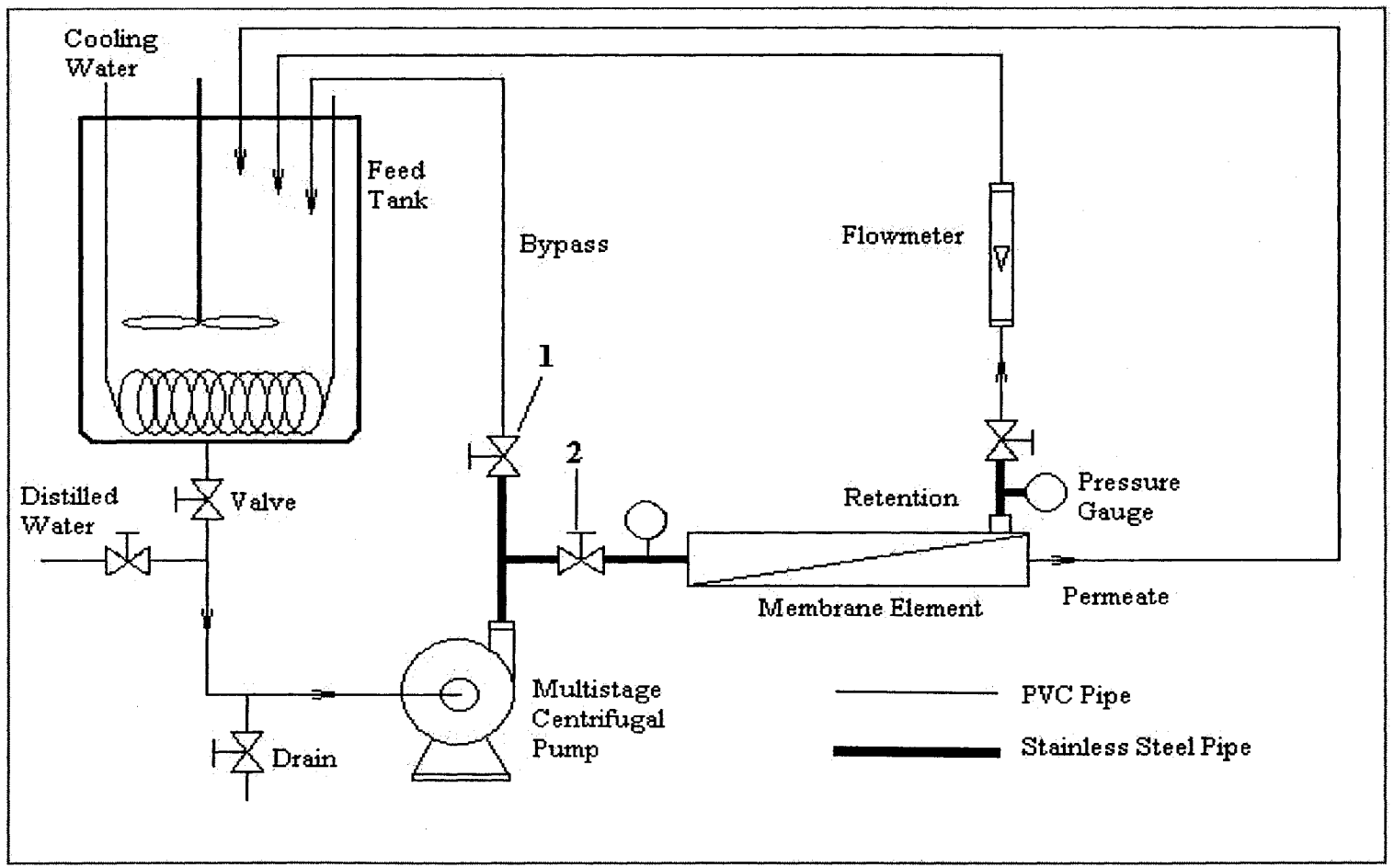

Figure 3-1 Flowchart of experimental set-up

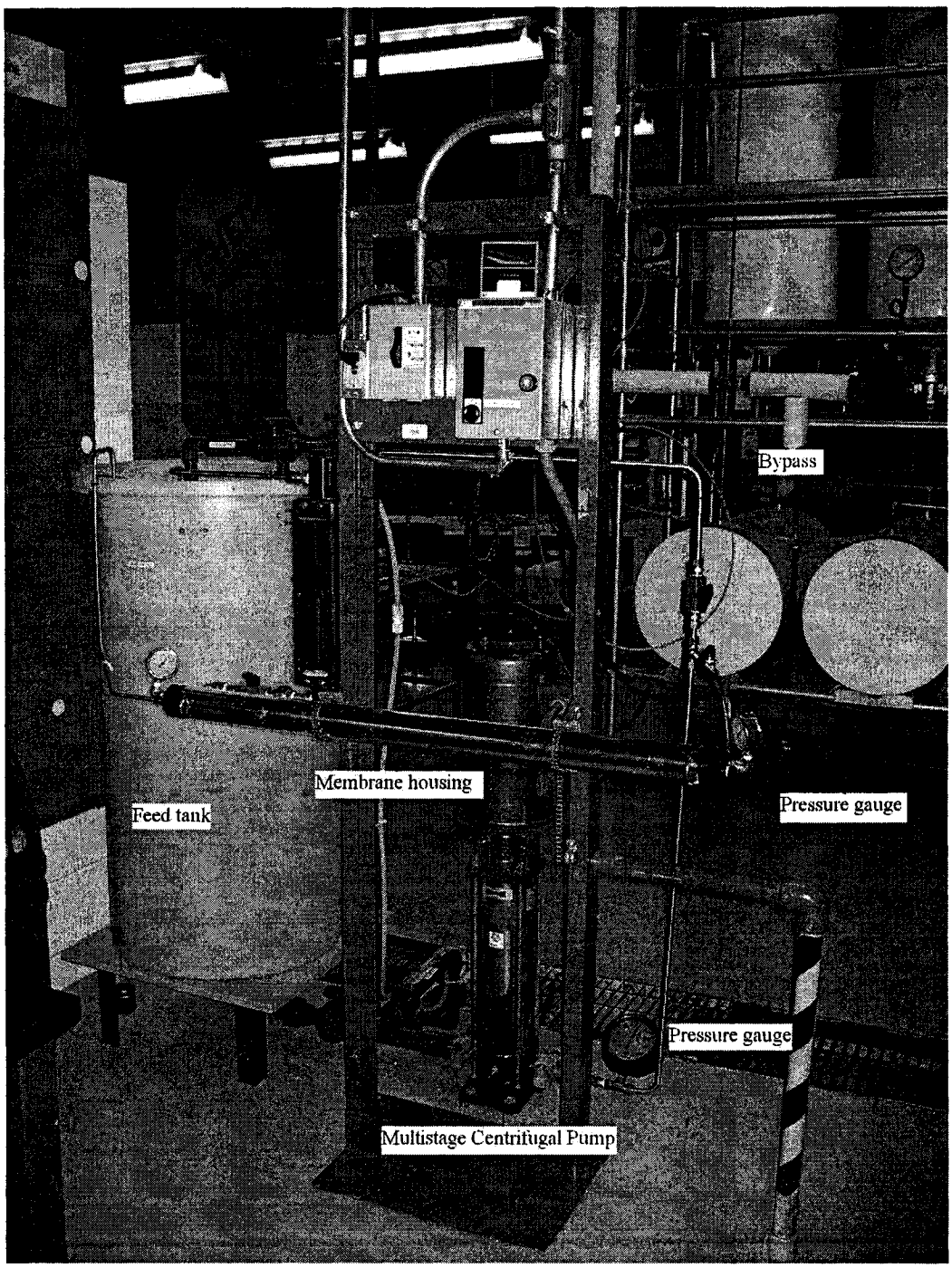

Figure 3-2 Photo of experimental setup

Pressure gauges were placed at the beginning and the end of the membrane housing. The inlet pressure of membrane elements was controlled by manipulating the two valves (valve 1, 2, see Figure 3-1) located on the bypass, feed stream lines. The flowrate of retention stream was measured using a liquid flowmeter and that of the permeate stream was measured manually using a graduated cylinder and a stopwatch. Feed flowrate was calculated as the sum of the flowrates of retention and permeate streams. Cooling coil was submerged under the feed solution in the feed tank to maintain the pre-set temperature using tap water.

The experimental system was constructed from stainless and polyvinyl chloride plastic (PVC) pipe. During the early tests, rust was found in the feed solution. In order to prevent this phenomena and fouling on membranes, all piping in the system was replaced with high grade stainless tubing.

The experimental system was installed in the Department of Chemical Engineering at the University of Ottawa.

3.4 Experimental procedure

For each run, feed solution containing appropriate concentrations of sodium chloride and sodium sulfate was pumped from the feed tank to the membrane housing which NF membrane element was assembled inside. After the steady state for set operating condition of temperature, pressure and flowrate was reached, measurements and samplings were conducted.

3.4.1 Constant feed concentration tests

In the experimental setup shown in Figure 3-1. Since the permeate, retentate and bypass stream were returned back to feed tank, the total volume of the solution remains unchanged, the feed concentration can be considered as a constant. The purposes of constant feed concentration tests is to study the infuence of membrane type and operating conditions such as pressure, temperature, and feed flowrate on the performance of the separation processes. Feed solution was the synthetic brine containing 200g/L sodium chloride (NaCl) and 10 g/L sodium sulfate (Na_2SO_4). Other conditions will be indicated in the relevant texts in the Results and Discussion section.

3.4.2 Volume reduction tests

The purpose of volume reduction tests was to simulate the industrial desulphurization craft condition by using NF membrane element. In an industrial scale sulfate removal membrane system, membrane elements are placed one after another inside the housing, with the feed flowing through the membrane elements and the sulfate concentration increasing from entrance to the end of the membrane housing. Therefore we should determine the effects of feed concentration on membrane performance, such as on rejection and permeate flux to provide the guidelines for industrial design.

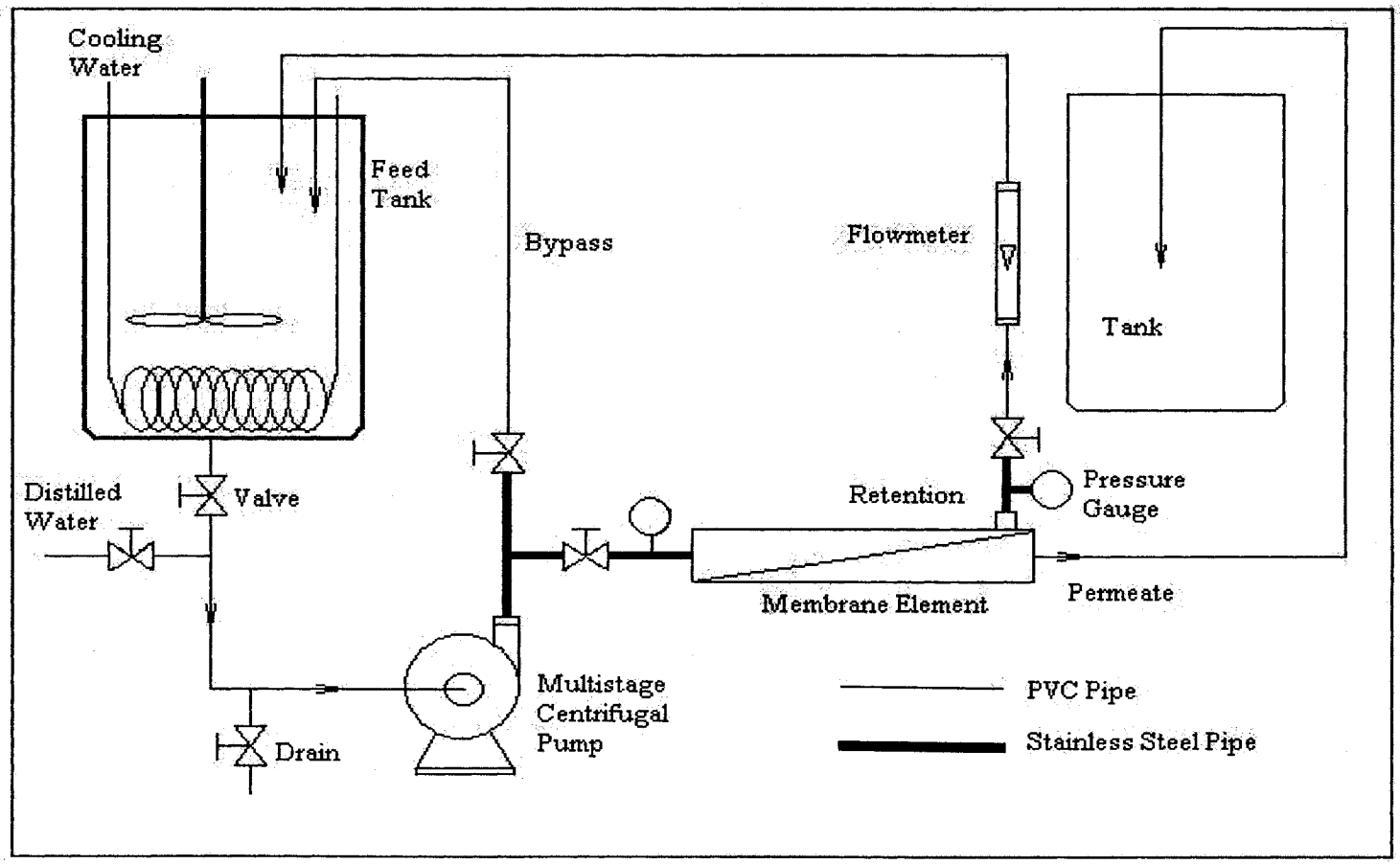

Figure 3-3 Flowchart of volume reduction test set-up

The volume reduction tests were performed with experimental set-up shown in Figure 3-3. The difference between this setup from that shown in Figure 3-1 was that the permeate stream was collected with separated tank, not returned back to the feed tank. With the taking off permeate, the volume of feed solution was decreased and the concentration of solution increased gradually.

Two kinds of membrane elements (NF270-2540 model by FilmTec (DOW) and DL2540F model by GE Osmonics) were investigated in the volume reduction test. The following steps were carried on: in each run, the system was first set to the required temperature, pressure, feed flowrate with appropriate feed brine and stabilized for 30 minutes by recycling both permeate and retention stream back to the feed tank. Performance parameters such as pressure drop and flux were then measured and recorded accordingly. Samples were taken for later measurement of sodium sulfate concentration and sodium chloride concentration in permeate and retention streams. Then, a volume of permeate equivalent to 15% of the original feed volume was collected separately. The remaining retention was used as the feed brine for the next run. All the volume reduction experiments were conducted at temperature of 45 °C.

4. Analytical methods

4.1 Analytical method of sulfate

Sulfate concentration was measured using a turbidimetric method. The principle of this method is when adding barium ion into the sulfate solution, sulfate ion is converted to a barium sulfate suspension under controlled conditions. The resulting turbidity was determined by a spectrophotometer and compared with a curve prepared from standard sulfate solution.

The procedure for turbidimetric measurement were: first, samples diluted to an appropriate concentrations were mixed with 10 ml distilled water and 5 ml conditioning reagent in a 100 ml beaker, mixed well by gentle stirring with a magnetic stir; then, about 0.1-0.2 g of $BaCl_2$ was added to the beaker; after gentle stirring for exactly one minute, 1 ml of the suspension was transferred to a corvette; the turbidity of the suspension was measured exactly five minutes after the transfer using a DU Series 600 spectrophotometer (Bechman Instruments Canada Inc.). The conditioning agent was prepared by mixing 50 ml glycerol with a solution containing 30 ml concentrated HCl solution. The concentrated NaCl solution was prepared by dissolving 100 ml isopropyl alcohol and 75 g NaCl in 300 ml distilled water.

4.2 Analytical method of chloride

The operation of a chloride electrode is based on the potential which develops across a silver chloride membrane. This potential is proportional to the activity of chloride

ions in contact with membrane. The relationship between potential and chloride ion activity is expressed by the Nernst Equation:

$$E = E^0 - S \cdot \log A \qquad (4\text{-}1)$$

where

E = measured electrode potential

E^0 = constant, the sum of several system potentials

S = electrode slope

A = Chloride ion activity

At 25 °C, the ideal Nernstian slope is -59.2mV per decade increase in chloride ion activity

The chloride ion activity is related to chloride concentration as follows:

$$a = \gamma_k \cdot c \qquad (4\text{-}2)$$

where

a = activity

γ_k = activity coefficient

c = concentration

The activity coefficient γ is dependent on and can be estimated from the total quantity of ions in solution, i.e., ionic strength. Ionic strength is an essential concern when

using ion selective electrodes. In very dilute solutions, the activity coefficient approaches a value of one, and activity and concentration are the same.

In this experiment, the concentration of sodium chloride was measured using a chloride Ion Combination Glass Electrode (Fisher Scientific) coupled with a dual channel PH/Ion/Conductivity Meter, Model AR 50 (Fisher Scientific).

5. Results and discussion

This section describes effects of operating parameters such as pressure, temperature and feed flowrate on membrane performance in terms of permeate flux, sulfate rejection and chloride passage based on experimental data.

5.1 Constant feed concentration tests

Based on the information from manufacture, three membrane elements, i.e. NF 270-2540 membrane element of FilmTec Corporation, DL 2540F membrane element of GE Osmosis and XN 45-2540 membrane element of TriSep Corporation - were selected for performance testing. A series of tests were conducted to study the effects of operating parameters on sulfate rejection, chloride passage, and permeate flux of different membrane at constant feed concentration. Experimental data are listed in appendices tables.

5.1.1 Effects of operating temperature

This section discusses the effects of operating temperature on the selective sulfate removal of different membrane elements at different temperature under of constant pressure and feed flowrate.

5.1.1.1 Effect of temperature on sulfate rejection

The experiments were carried out with the temperature in the range from 25 °C to 40 °C using the three types of membrane elements with feed brines containing 200 g/L sodium chloride and 10 g/L sodium sulfate. A constant condition of 50 psig pressure and 2 GPM feed flowrate was maintained during the run. Experimental results of sulfate rejection vs temperature was plotted in Figure 5-1.

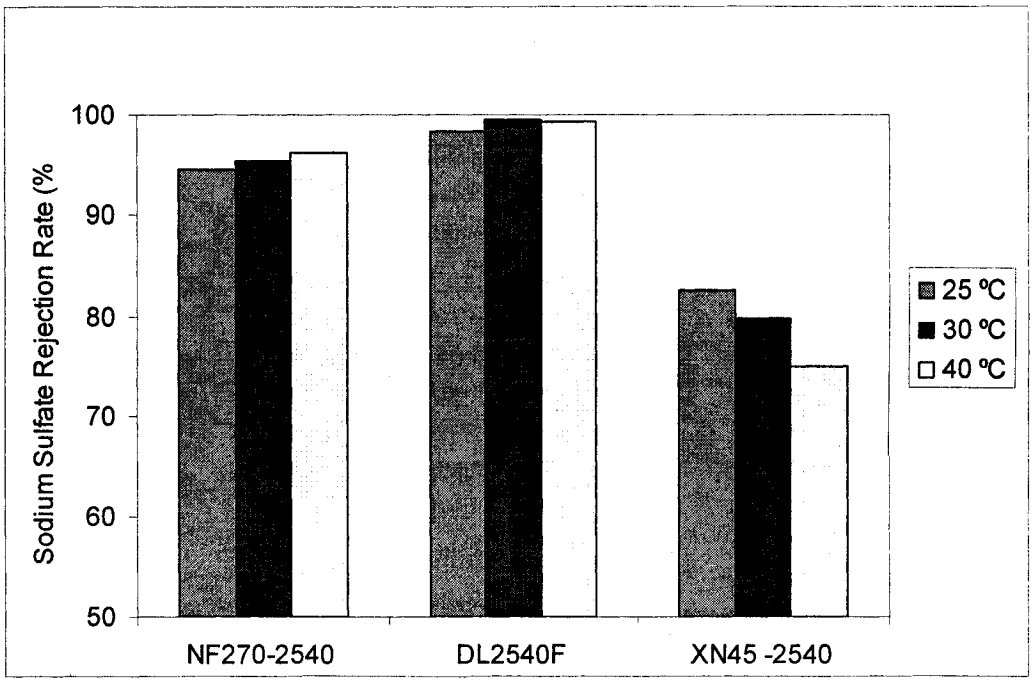

Figure 5-1 Plot of sulfate rejection vs temperature for different membrane elements (pressure 50 psig)

As shown in Figure 5-1, the NF 270-2540 membrane element of FilmTec showed a slight increase in sulfate rejection from 95.5% to 96.9% as temperature increased from 25 to 40°C. The sulfate rejection for DL 2540F membrane element of GE Osmonics remained almost unchanged at a high level of 97% to 99% in the same temperature range. On the other hand, XN 45-2540 membrane element of TriSep showed substantial decrease of sulfate rejection decreased from 82.6% to 75.0% when

operating temperature increased from 25 to 40 °C. Furthermore, the sulfate rejection of XN45 was significantly lower than that of the other two membranes in the tested temperature range.

The differences of sulfate rejection of the three membranes may be due to the differences of molecular weight cut off of three membranes. As shown in Table 1, the molecular weight cut off range of DL2540F, NF270-2540 and XN45-2540 membranes are 150-300, 200-300 and 500-1000 Da, respectively. showing that the molecular cutoff ranges of DL2540F and NF270-2540 membranes are closer to hydrated sulfate size than XN45-2540 membrane.

From the sulfate rejection point of view, it can be summarized that DL 2540F and NF 270-2540 membrane elements are more suitable than XN45-2540 membrane element for sulfate removal of chloralkali brine because they have higher sulfate rejection.

5.1.1.2 Effects of temperature on chloride passage

Experimental condition was set as pressure 50 psig, feed flowrate = 2 GPM, feed brines containing 200 g/L sodium chloride and 10 g/L sodium sulfate. Experiment were carried out and samples were collected with the temperature increased from 25 °C to 40 °C during the runs, the experimental data of chloride passage vs temperature was plotted in Figure 5-2

DL25450F and NF 270-2540 membrane elements showed high passage of sodium chloride as the temperature increased from 25 °C to 40 °C, chloride passages of

NF270-2540 membrane were over 92%, and chloride passage range of DL2540F membrane element was from 86.6% to 93.6%. The data inconsistencies were probably due to experimental errors but still in the industrially acceptable range, XN45-2540 membrane element showed consistently low chloride passage.

From the chloride passage point of view, it is also clear that NF 270-2540 and DL 2540F membranes are more suitable than XN45-2540 membrane for the application in sulfate removal from chloralkali brine because their significantly higher chloride passage would allow a more efficient recovery of sodium chloride (Figure 5-2).

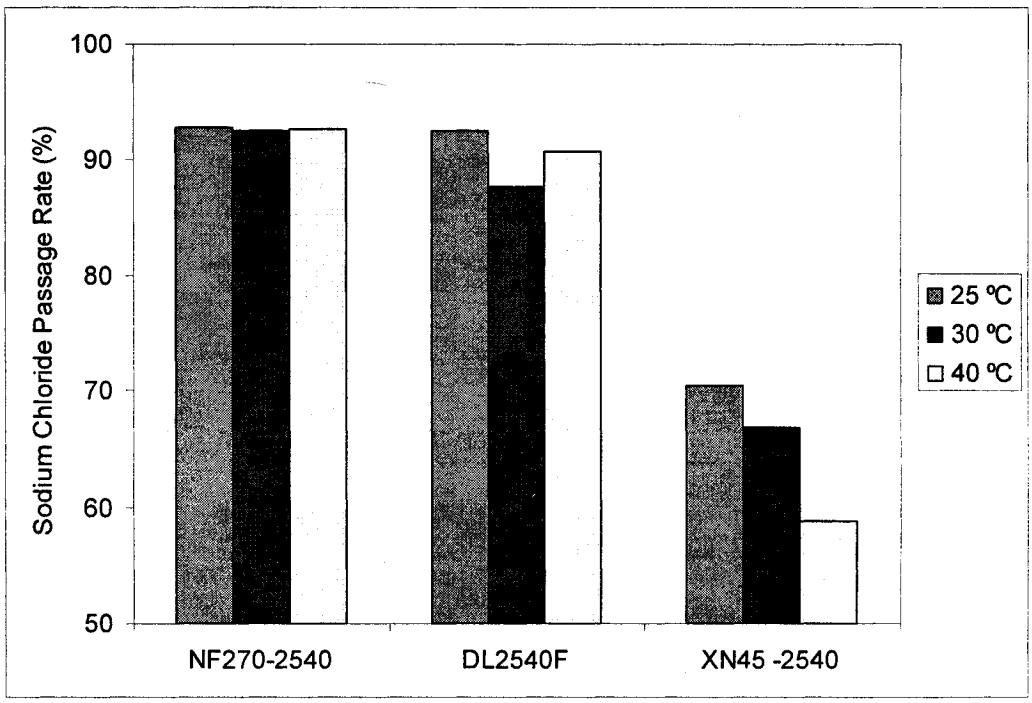

Figure 5-2 Plot of chloride passage vs temperature for different membranes

5.1.1.3 Effects of temperature on permeate flux

The effects of temperature on membrane permeate flux was also studied experimentally because permeate flux determines the throughput of an industrial process. It also has a direct influence on the solute rejection of an NF membrane process as indicated by Arrhenius equation, which will be discussed later.

A temperature close to 80 °C would be most favorable for a sulfate removal membrane process for chloralkali facilities because the brine temperature from a chloralkali facility that is subject to the sulfate removal process is approximately 80 °C. A processing temperature close to that would reduce the capital cost and energy consumption associated with the heat exchange of the brines. However, based on the specification of membrane products, the maximum operating temperatures for the three membranes are in the range of 45- 50 °C.

Experiments were conducted in the temperature range between 20 and 45 °C. Experiments were carried out at 100 psig pressure and 2 GMP feed flowrate with feed brines containing 200 g/L sodium chloride and 10 g/L sodium sulfate. Experimental results are shown in Figure 5-3. It can be observed from Figure 5-3 that the permeate flux increases with temperature, and the influence of temperature on permeate flux was due to the dependency of the viscosity of salt solution and follows the Arrhenius model as follows [88]:

$$J_v = J_0 \cdot \exp\left(-\frac{E_p}{RT}\right) \qquad (5\text{-}1)$$

where J_v is volumetric permeate flux; J_0 pre-exponential factor; E_p the apparent activation energy for permeation; R the gas constant and T the absolute temperature.

Rearranging Eq. (5-1) gives following linear relationship:

$$\ln J_v = \ln J_0 - \frac{E_p}{RT} \tag{5-2}$$

Plot $\ln(J_v)$ vs $1/T$, we can get Figure (5-3) below. It can be seen that there is a linear relationship between $\ln(J_v)$ and $1/T$, confirm that Arrhenius model is applicable for this case.

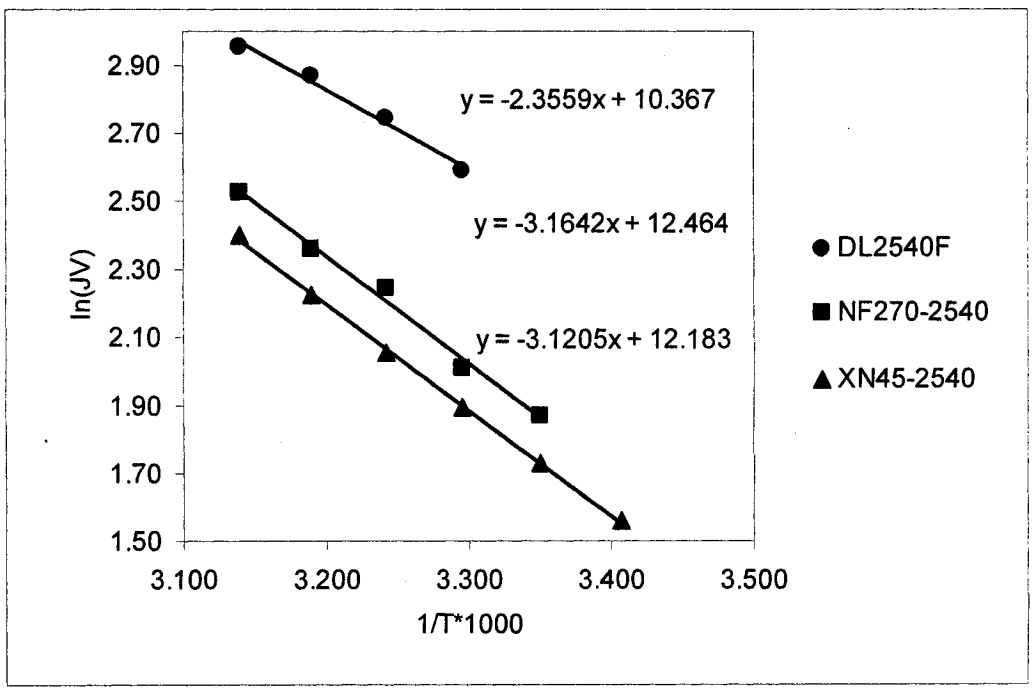

Figure 5-3 Permeate flux as a function of temperature (operating pressure at 100 psig, feed flowrate at 2 GPM)

The experimental results of permeate flux as a function of temperature is shown in Figure 5-3 above. The experimental results confirm that for the three membrane elements tested, Arrhenius model can describe and fit the experimental data of the DL2540F, NF270-2540 and XN45-2540 membranes properly with slope of -2.3559, -3.1642 and -3.1205 respectively. The R-squared values for the three membranes are all over 0.99. From Figure 5-3, the pre-exponential factor J_0 and the apparent activation energy E_p for three membranes can be obtained. The values of these parameters are listed in Table 5.1.

Table 5-1 Pre-exponential factor and the apparent activation energy for three membranes

Membrane type	Pre-exponential factor J_0	the apparent activation energy E_p
DL2540F	3.18×10^4	2.36×10^3
NF270-2540	2.59×10^5	3.16×10^3
XN45-2540	1.95×10^5	3.12×10^3

As shown in Table 5-1, DL2540F membrane element showed the lowest apparent activation energy and the highest value of the pre-exponential factor, which corresponds to the largest fluxes of this membrane among the three NF membrane elements in the tested temperature range. On the other hand, the permeate flux of NF270-2540 is slightly higher than that of XN45-2540 membrane elements.

5.1.2 Effects of operating pressure

This section discusses the effects of operating pressure on membrane performance under constant temperature and feed flowrate.

5.1.2.1 Effects of operating pressure on sulfate rejection

Experiments were carried out to study the effects of operating pressure on sulfate rejection. The operating pressure was varied from 50 to 150 psig, while all other conditions were kept constant. Figure 5-4 shows the dependency of sulfate rejection of the three membranes on operating temperature at temperature of 45 °C and feed flowrate of 4 GPM. The feed solution contained 200 g/L NaCl and 10 g/L Na_2SO_4. Test results of relation between sulfate rejection and operating pressure was plotted in Figure 5-4. The results indicate that under the specified pressure range of 50 to 150 psig, pressure did not have significant influence on sulfate rejection for all the three membranes. DL2540 and NF270-2540 membrane elements had high sulfate rejections from 97% to 99%. Still, XN45-2540 showed low sulfate rejection at the experimental condition as compared to DL2540 and NF270-2540 membranes. Variation of the operating pressure would affect the permeate flow rate. An increase in operating pressure results in increase of driving force for the solvent, but only marginally affects the driving force for the solute.

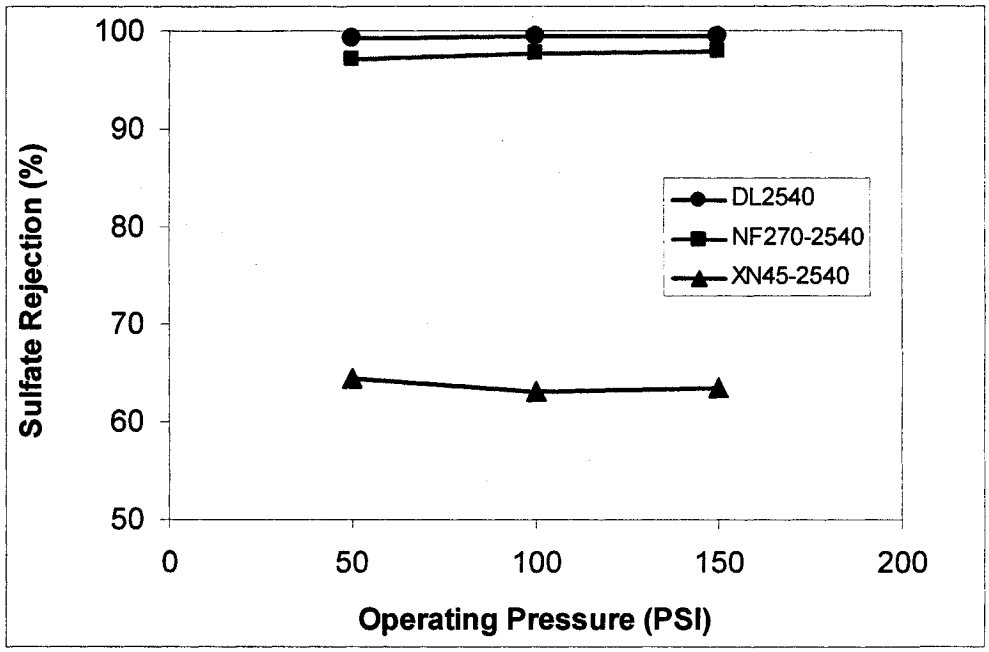

Figure 5-4 Plot of Sulfate rejection vs operating pressure (Temperature at 45 °C, Feed flowrate at 4 GPM)

5.1.2.2 Effects of operating pressure on chloride passage

Tests were carried out to study the effects of operating pressure on chloride passage at the same condition as that of the tests of sulfate rejection, which was operating at temperature of 45 °C and feed flowrate of 4 GPM. The feed solution contained 200 g/L NaCl and 10 g/L Na_2SO_4.

Effects of operating pressure on chloride passage for the three NF membrane elements were conducted experimentally. Results are shown in Figure 5-5 according the measurement of chloride concentration in permeate and feed samples. The concentration of feed solution contained 200 g/L NaCl and 10 g/L Na_2SO_4. The results indicate that under the tested temperature and feed flowrate conditions, with

the pressure changing from 50 to 150 psig, operating pressure did not have significant influence on chloride passage for all the three membranes. As can be seen from Figure 5-5, under the tested conditions, the chloride passage of both DL2540F and NF270-2540 membrane elements was more than 90%, the chloride passage of DL2540F membrane varied from 92.7% to 95.2%, that of NF270-2540 increased slightly from 90% to 96.7%. XN45-2540 membrane showed low chloride passages from 63.1% to 65.6%.

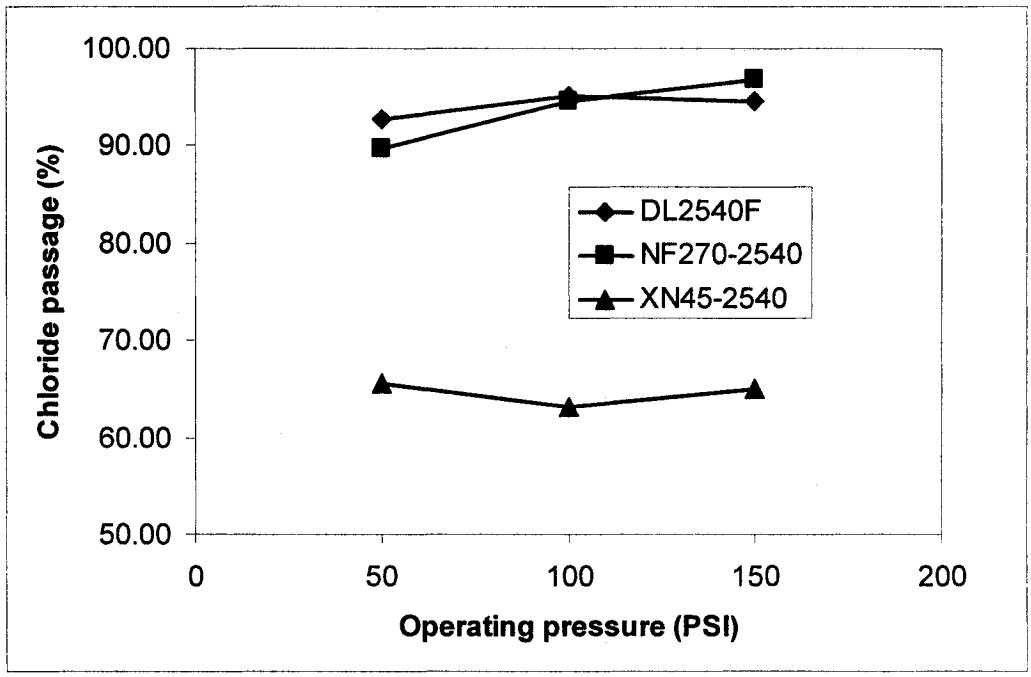

Figure 5-5 Plot of chloride passage vs operating pressure (Temperature: 45 °C, Feed flowrate: 4 GPM)

The above experimental results suggest that DL2540F and NF270-2540 membrane elements are superior to NX45-2540 in terms of sulfate selectivity

5.1.2.3 Effects of pressure on permeate flux

An increase in permeate volumetric flux was observed as the pressure was increased. The effects of operating pressure on permeate fluxes of DL2540F, NF270-2540 and XN45-254 membranes at 40 °C and 4 GPM feed flowrate are presented in Figure 5-6. The feed brine contained 200 g/L sodium chloride and 10 g/L sodium sulfate. As can be seen from Figure 5-6, in the tested pressure range from 50 psig to 150 psig, DL2540F membrane has highest permeate flux compare with other two membranes. The permeability of NF270-2540 is slightly high than that of XN45-2540 membranes. The permeate flux increased linearly with the operating pressure increasing for both membrane elements. This linearity between the permeate flux and the operating pressure would imply that the change of osmotic pressure across the membrane due to the change of operating pressure was not significant. This is reasonable because the change of sodium sulfate concentration at membrane interface due to sulfate polarization at the tested pressure range was not significant.

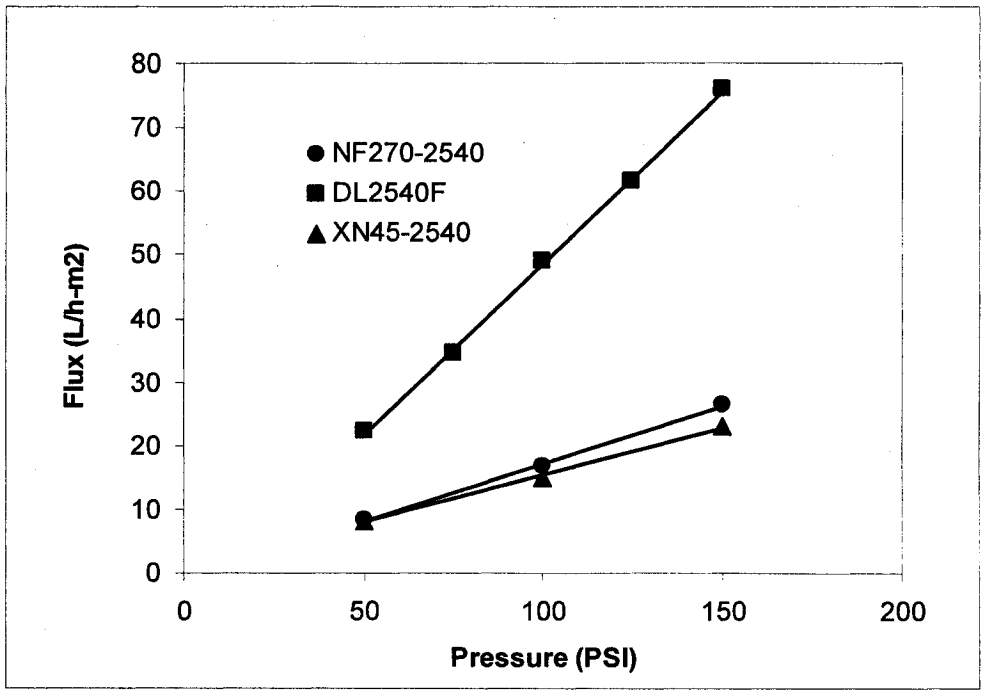

Figure 5-6 Plot of permeate flux vs operating pressure (temperature at 40 °C, feed flowrate at 4 GPM)

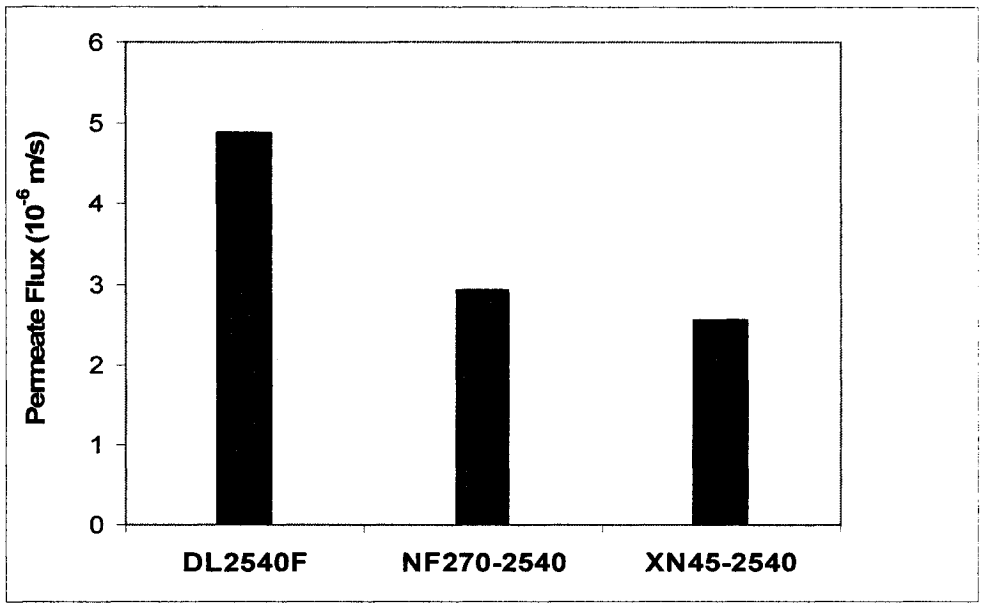

Figure 5-7 Permeate flux of three membrane elements at 40 °C

Volumetric permeate flux (J_V) can be calculated by the following equation:

$$J_V = \frac{Q_P}{A} \tag{5-3}$$

where Q_P is the volumetric flowrate of permeate and A the active membrane area.

According to Equation (5-3), the slope of the linear flux vs pressure curves are the membrane permeability of different membranes at the tested conditions, which were 0.5383 and 0.1825 $l/h \cdot m^2 \cdot PSI$ for DL2540F membrane and NF270-2540 membrane respectively. Considering the fact that DL2540F membrane and NF270-2540 membrane have very similar selectivity, this result recommended that DL2540F membrane is more suitable than NF270-2540 membrane element for sulfate removal from chloralkali brine because under the same pressure and temperature, DL2540F membrane element offers higher permeate flux.

5.1.2.4 Relationship between the pressure drop along membrane element and feed flowrate

Tests were performed to study the relationship between pressure difference (pressure drop) on the two ends of a membrane element and feed flowrate at 150 psig pressure

and 45 °C temperature using NF270-2540 and DL2540F membrane elements. The concentration of feed solution contained 200 g/L NaCl and 10 g/L Na_2SO_4. Experimental results are shown in Figure 5-8 below. It can be observed that pressure drop increased with the increase of feed flowrate.

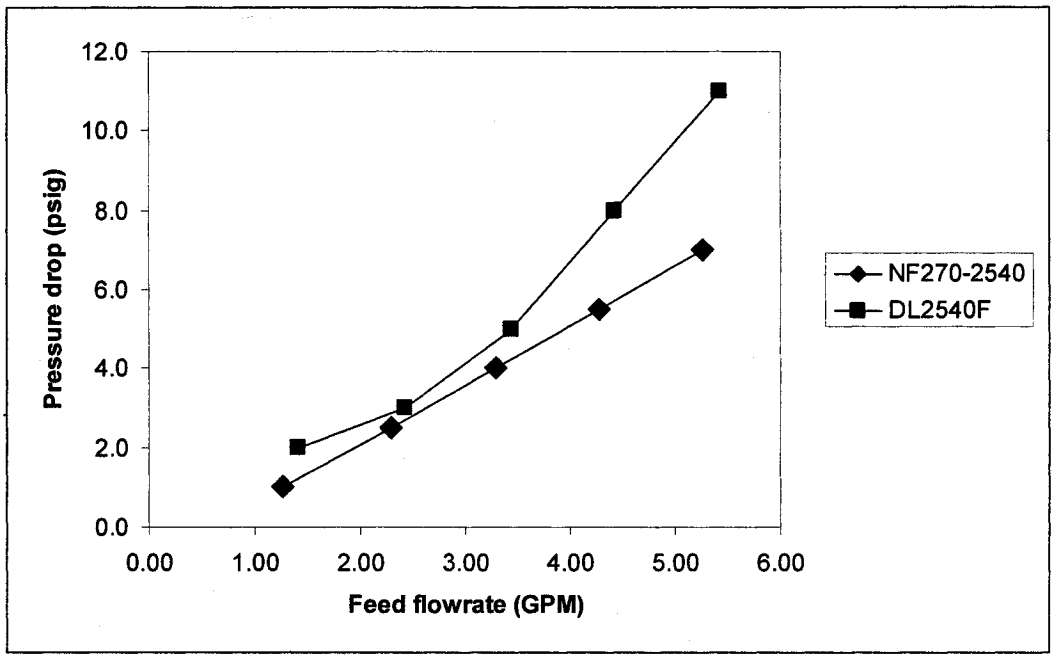

Figure 5-8 Relationship between pressure drop and feed flowrate

By hydrodynamic theory, the pressure drop over the membrane element module is due to the frictional resistance, and the frictional resistance can be obtained based on the flow regime and the geometry of the channel in membrane element. In this case, because the flow regime inside the membrane module was running in the turbulent flow regime, so the pressure drop over the membrane module can be obtained from the Fanning model which indicates that that pressure drop increased with the increase of feed flowrate.

5.2 Volume Reduction Test

The first objective of volume reduction tests was to investigate the effects of feed concentration on membrane performance. The second objective was to simulate chloralkali industrial sulfate removal conditions by using a single membrane element.

In the volume reduction experiments, for each run, 15% volume of permeate of the initial feed volume was collected in a separate tank. The remaining retention was used as the feed of the next run. The initial volume of the feed of the next run was thus 85% of the previous run, and the sodium sulfate concentration would be 10 – 15% higher, depending on the sulfate rejection rate in the previous run.

These tests were performed using the experimental setup shown in Figure 3-2 to study the effects of feed concentration on membrane performance using NF270-2540 and DL2540F membrane elements at 150 psig pressure, 45 °C temperature and 4 GPM feed flowrate.

5.2.1 NF270-2540 membrane element tests

Volume reduction tests were carried out with initial feed concentration of 10 g/l sodium sulfate and 200 g/l sodium chloride. In experiment, with the increasing of feed concentration, permeate flux became smaller and smaller, tests finished at feed sulfate

concentration of 56 g/l which permeate flux was really low and not applicable for industrial purpose. For all runs, the temperature was controlled at 45 °C, the feed flowrate at 4 GMP and pressure 150 Psig.

5.2.1.1 Selective sulfate removal: chloride passage and sulfate rejection

The volume reduction test of DL2540F membrane element was performed to study sulfate rejection and chloride passage. Sodium sulfate concentration in feed increased with the number of runs due to decreasing of feed volume by taking off permeate. The effect of feed concentration on permeate concentration (sodium sulfate) can be seen in Figure 5-9, permeate concentration increased significantly. While the feed concentration increased from 10 g/l to 58 g/l, accordingly feed concentration showed significant effect on sulfate rejection, which decreased from near 100% in the first run to 55% in the last run (Figure 5-10) under tested condition.

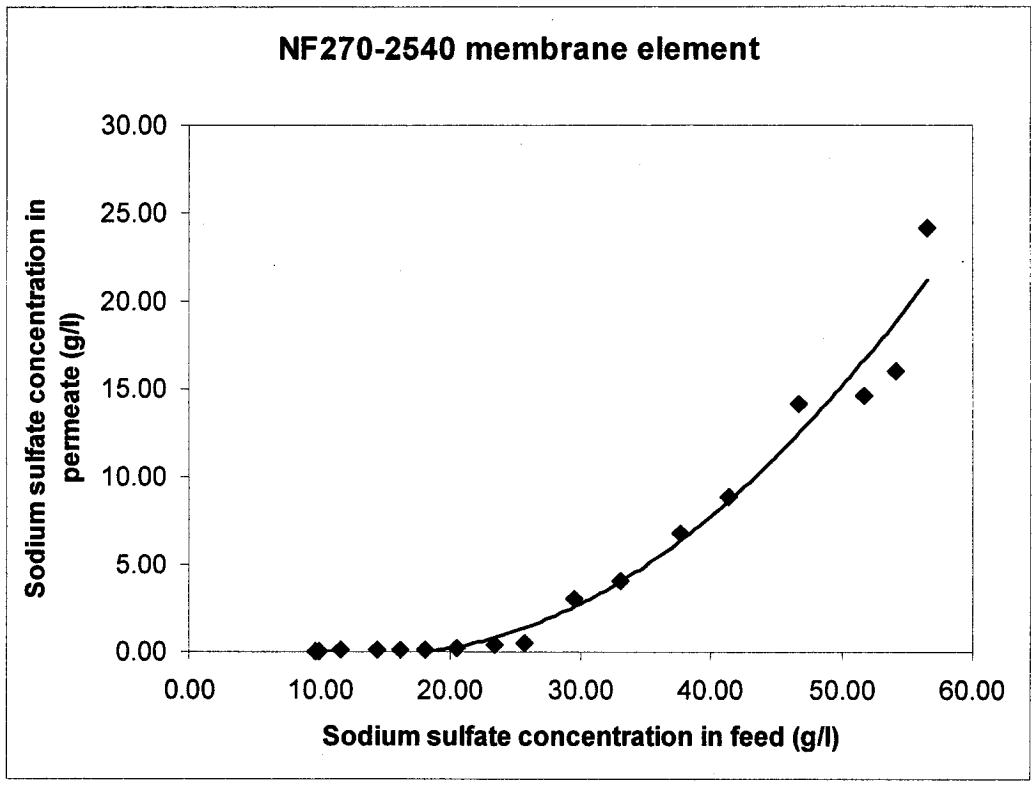

Figure 5-9 Plot of sodium sulfate concentration in feed vs sodium sulfate concentration in permeate

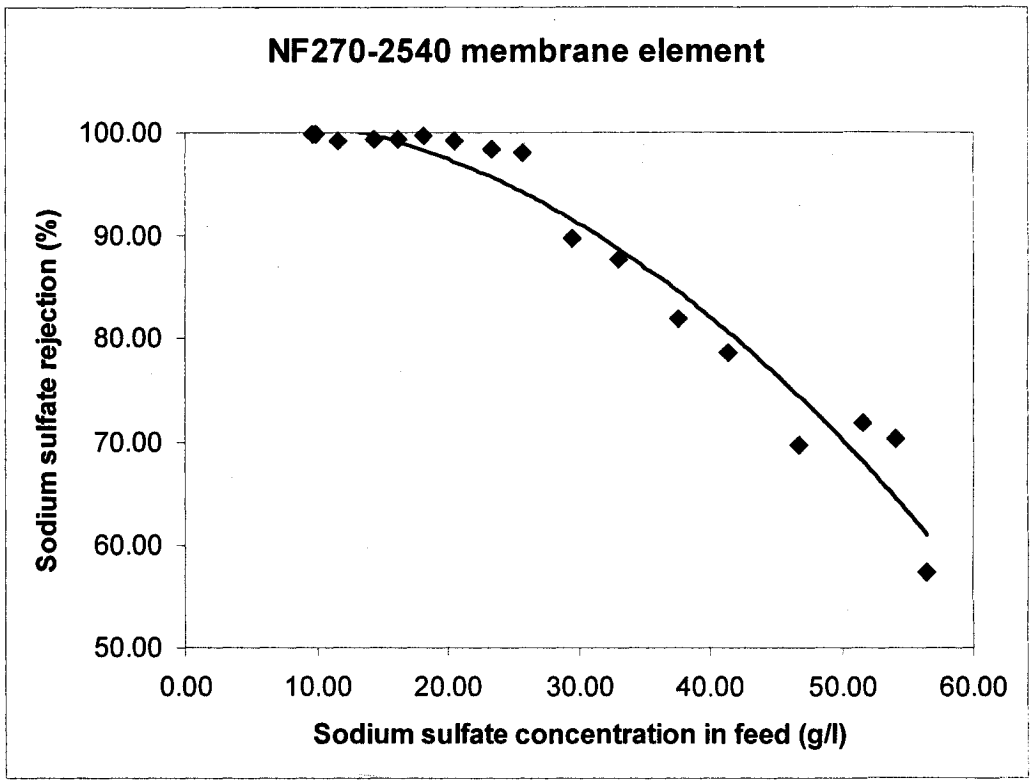

Figure 5-10 Plot of sodium sulfate concentration in feed vs sodium sulfate rejection

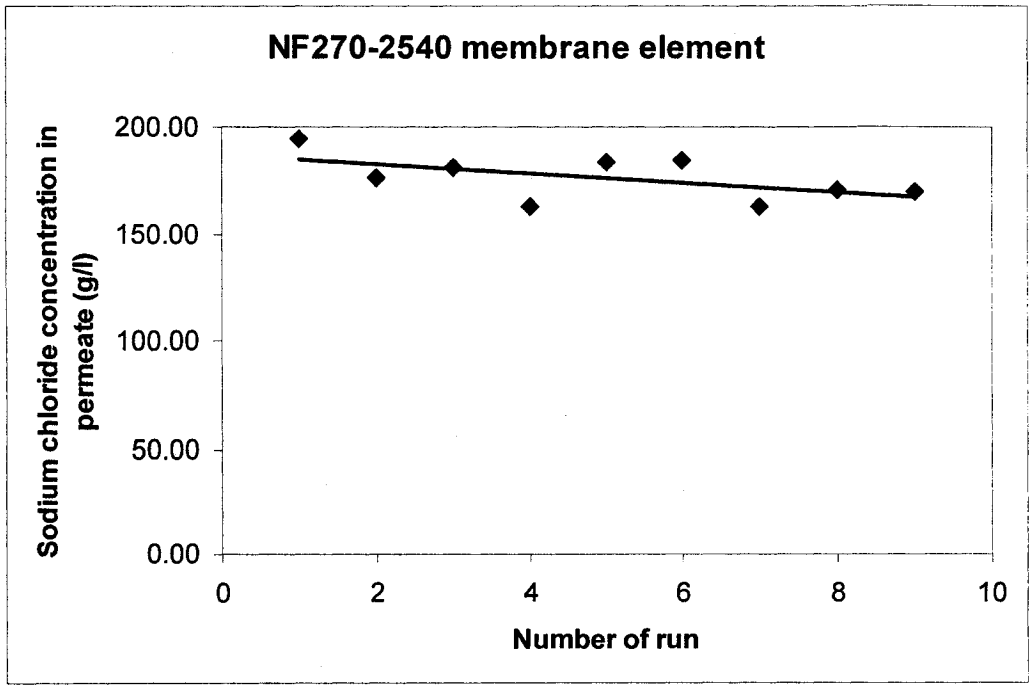

Figure 5-11 Plot of sodium chloride concentration in permeate vs number of run

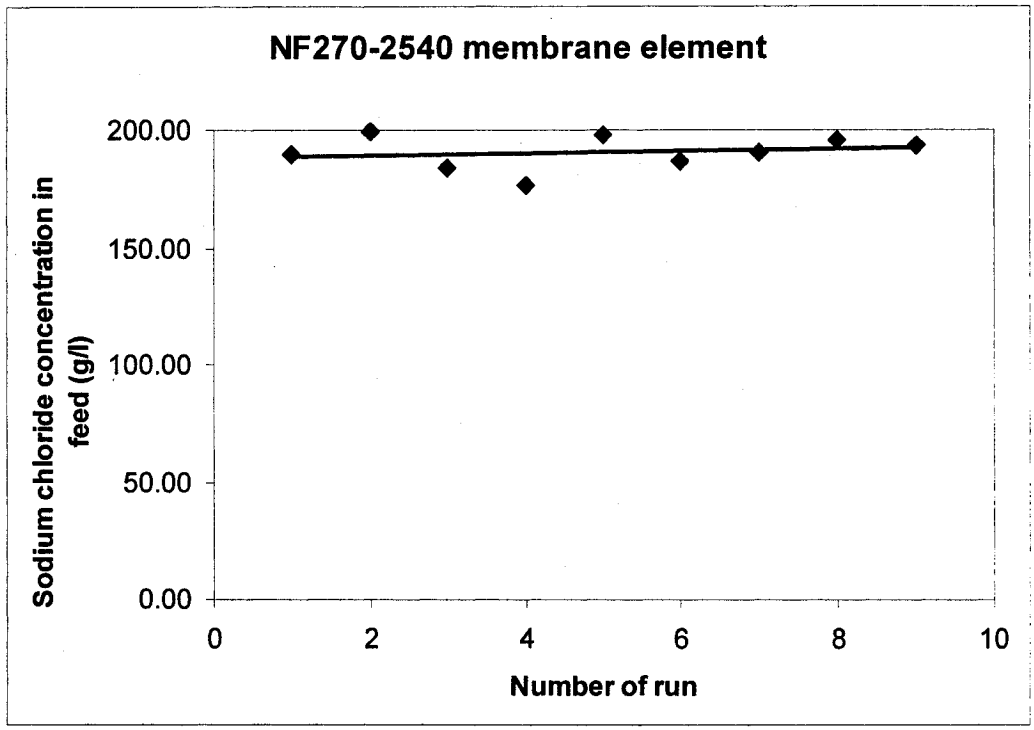

Figure 5-12 Plot of sodium chloride concentration in feed vs number of run

However, from Figure 5-11 and 5-12, it can be found that the sodium chloride concentration in feed, permeate, and retention were all high, indicating high chloride passage rate. Figure 5-13 below shows that chloride passage remained high with the increase of sodium sulfate concentration in feed. For all tests, the chloride passages meet the industrial requirement.

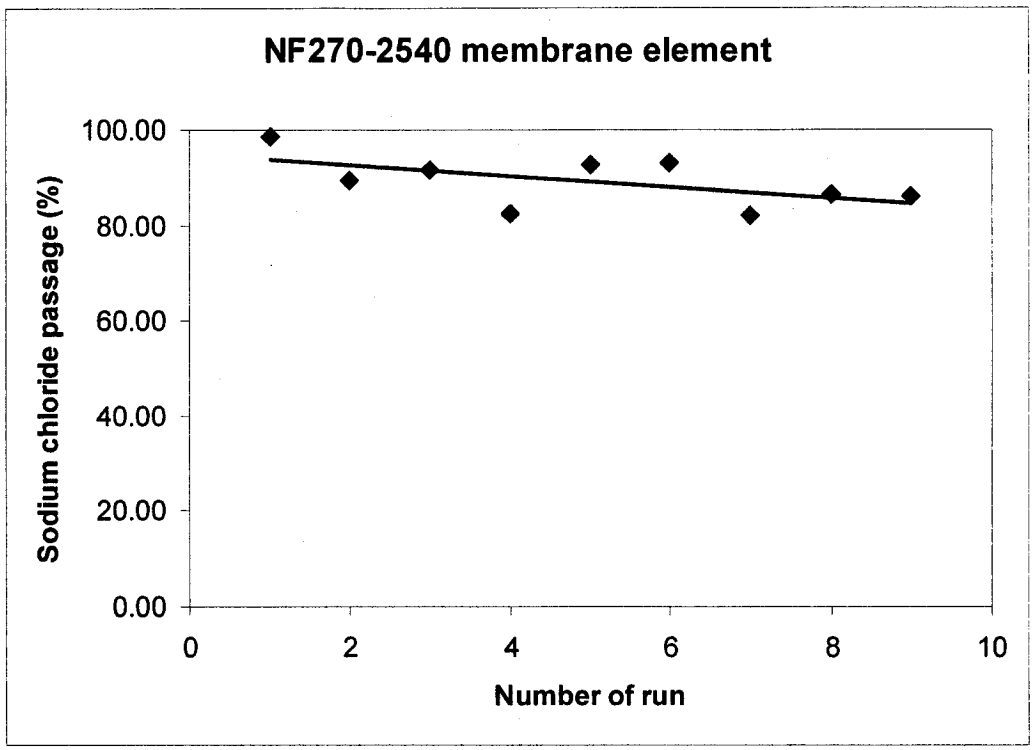

Figure 5-13 Plot of sodium chloride passage vs number of run

It can be concluded that NF270-2540 membrane element possesses excellent performance of selective sulfate removal (high rejection to sulfate and high passage to chloride) in low feed concentration range. However, the membrane performance deteriorated significantly with the increase of sulfate concentration in feed, but still can meet industrial requirement under the tested condition.

5.2.1.2 Effect of sodium sulfate concentration in feed on permeate flux

According to the results of the volume reduction experiments described above, a relationships of permeate flux and solute rejection with varying sodium sulfate concentration in feed concentration were established. Figure 5-14 shows the permeate

flux under different concentration of Na_2SO_4 in feed at constant pressure (100 Psig), temperature (45 °C), and feed flowrate (4 GPM). With the increasing of feed concentration, permeate flux became smaller and smaller. At 100 psig operating pressure, tests finished at feed sulfate concentration of 40 g/l because permeate flux was really low and not applicable for industrial purpose. Permeate flux declined with increase in concentration in feed at constant pressure (100 psig), temperature (45 °C) and feed flowrate (4 GPM). The results demonstrate that permeate flux declined significantly with increasing of sodium sulfate concentration in feed.

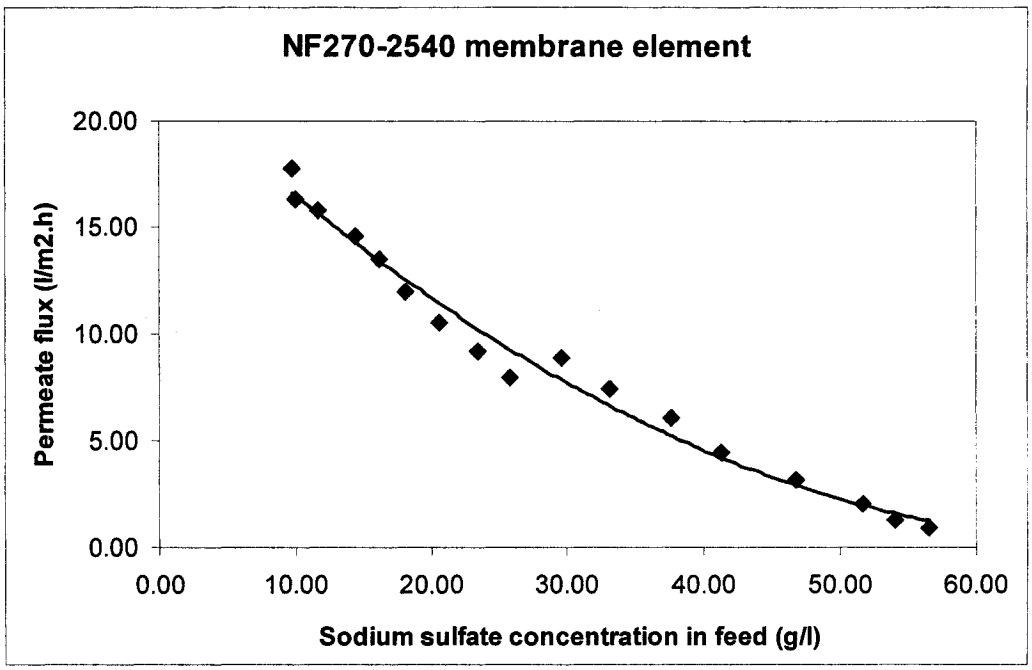

Figure 5-14 Plot of permeate flux vs sodium sulfate concentration in feed

5.2.1.3 Pressure drop along membrane element

Pressure drop along membrane element is also an important parameter for industrial membrane application because it will cause energy loss. As discussed previously, the

most important parameter that affects the pressure drop is the flow rate through membrane module. Figure 5-15 shows the dependency of pressure drop on feed flowrate at the sodium sulfate concentrations in feed of 9.35, 20.56, 33.13, 41.40, and 51.70 g/l, respectively. It can be seen that the pressure drop increased with the increasing of feed flowrate. Figure also shows that at the same feed flowrate, the pressure drop along the membrane element was larger with the later runs. This was because the sodium sulfate concentration in feed increased after each run, which resulted in the increase of bulk solution viscosity.

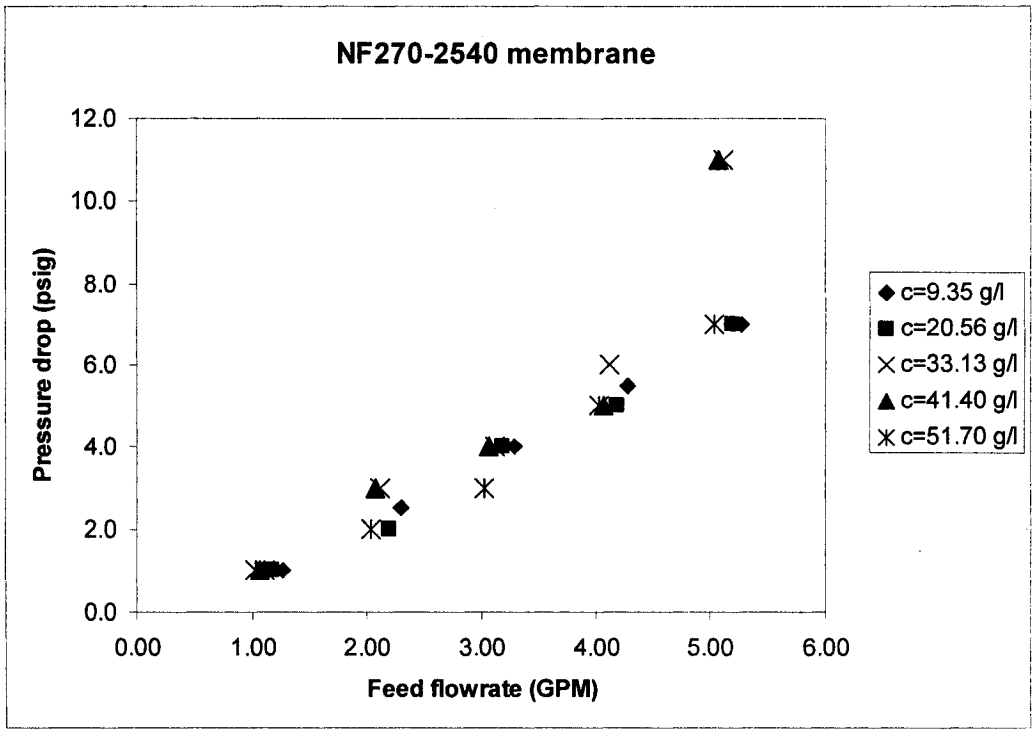

Figure 5-15 Plot of pressure drop vs feed flowrate for NF270-2540 membrane

5.2.2 DL2540F membrane element

5.2.2.1 Selective sulfate removal: chloride passage and sulfate rejection

Tests for DL2540F membrane element were carried out in the same experimental set-up (Figure 3-2) as NF270-2540. For all tests, the temperature was controlled at 45 °C, feed flowrate at 4 GMP and pressure at 100 Psig. Experiments were performed with initial feed concentration of 10 g/l sodium sulfate and 200 g/l sodium chloride, finished at feed concentration of 40 g/l sodium sulfate. Sodium sulfate concentration in feed vs sodium sulfate concentration in permeate was plotted in Figure 5-16.

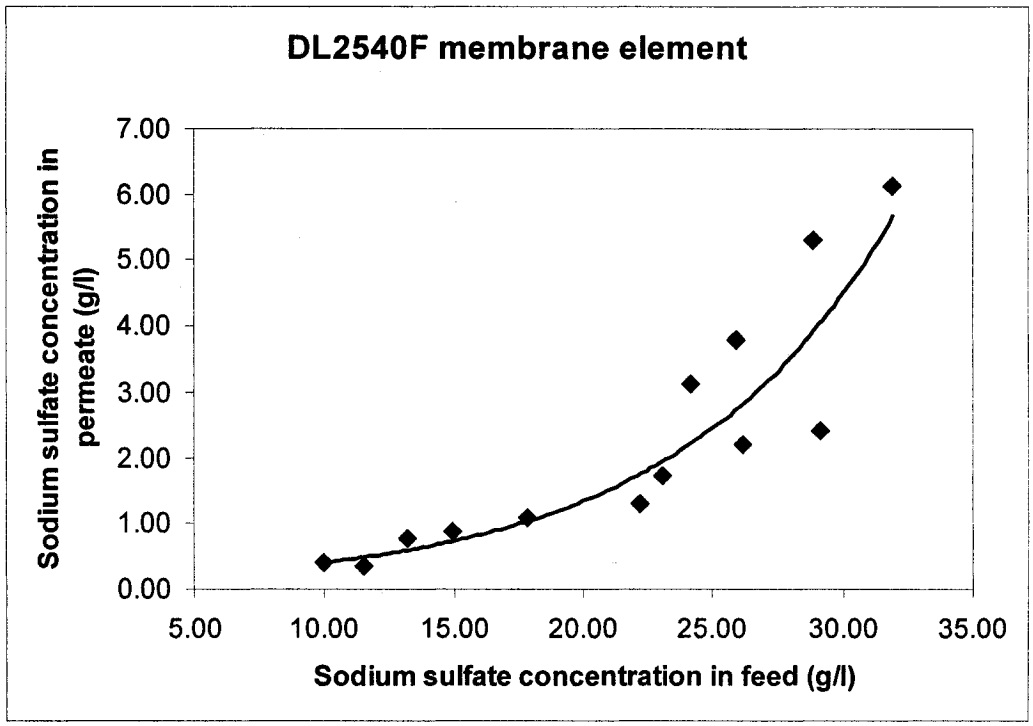

Figure 5-16 Plot of sodium sulfate concentration in feed vs sodium sulfate concentration in permeate

Sodium sulfate concentration in feed increased with the number of runs due to decreasing of feed volume by taking off permeate. As seen in Figure 5-16, sodium sulfate concentration in permeate increased significantly with the increase of sodium sulfate concentration in feed. Similarly, sodium sulfate concentration in feed also had significant affects on sodium sulfate rejection, which decreased significantly with the increase of sodium sulfate concentration in feed (Figure 5-17). Compare with NF270-2540 membrane (Figure 5-10), it can be found that DL2540F membrane has almost the same sulfate rejection rate at same operating condition. Form the sulfate rejection point of view, DL2540F and NF270-2540 membrane elements can be considered as favorable choices for the sulfate removal treatment of chloralkali brine.

Considering the sodium chloride passage, as shown in Figures 5-18 to 5-20, it can be seen that the sodium chloride concentration in feed and permeate were high in the range from 180 to 200 g/l, indicating high chloride passage rate. Figure 5-18 shows that sodium chloride concentration in permeate remained almost constant in all runs, indicating close to complete chloride passage under the investigated conditions. This is advantageous for industrial applications because the close to complete chloride passage would allow total recovery of sodium sulfate and low operating pressure.

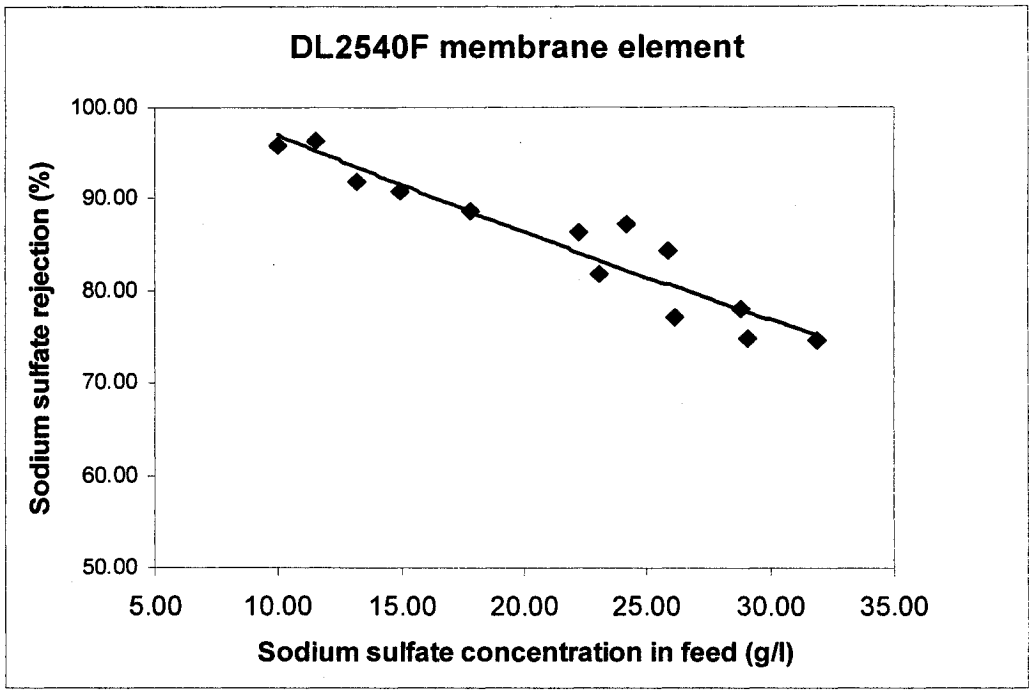

Figure 5-17 Plot of sodium sulfate concentration in feed vs sodium sulfate rejection

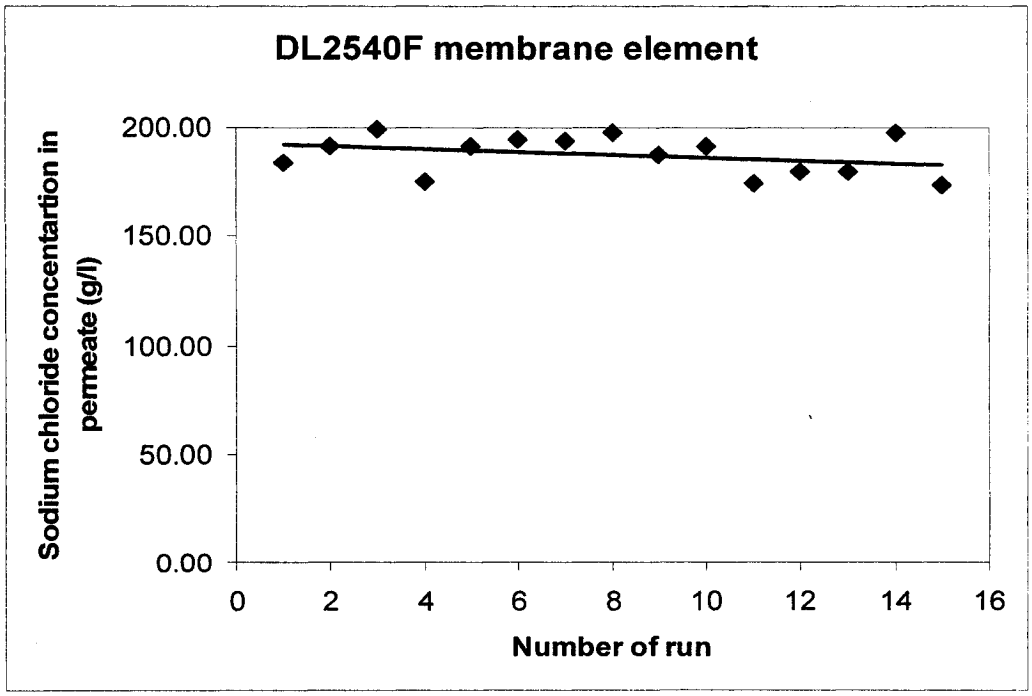

Figure 5-18 Plot of sodium chloride concentration in permeate vs number of run

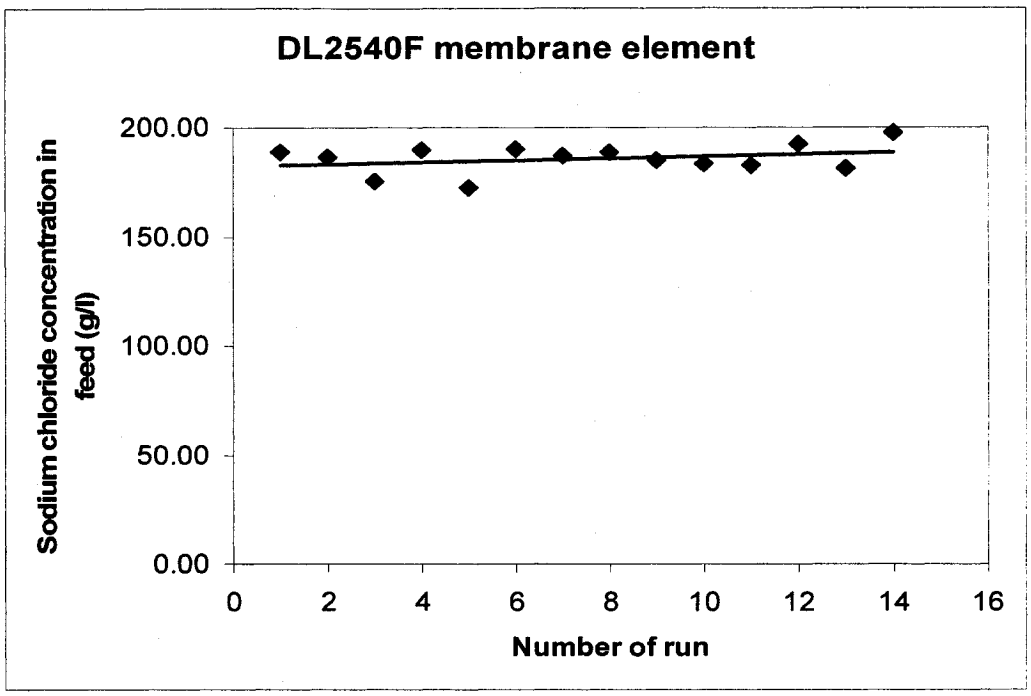

Figure 5-19 Plot of sodium chloride concentration in feed vs number of run

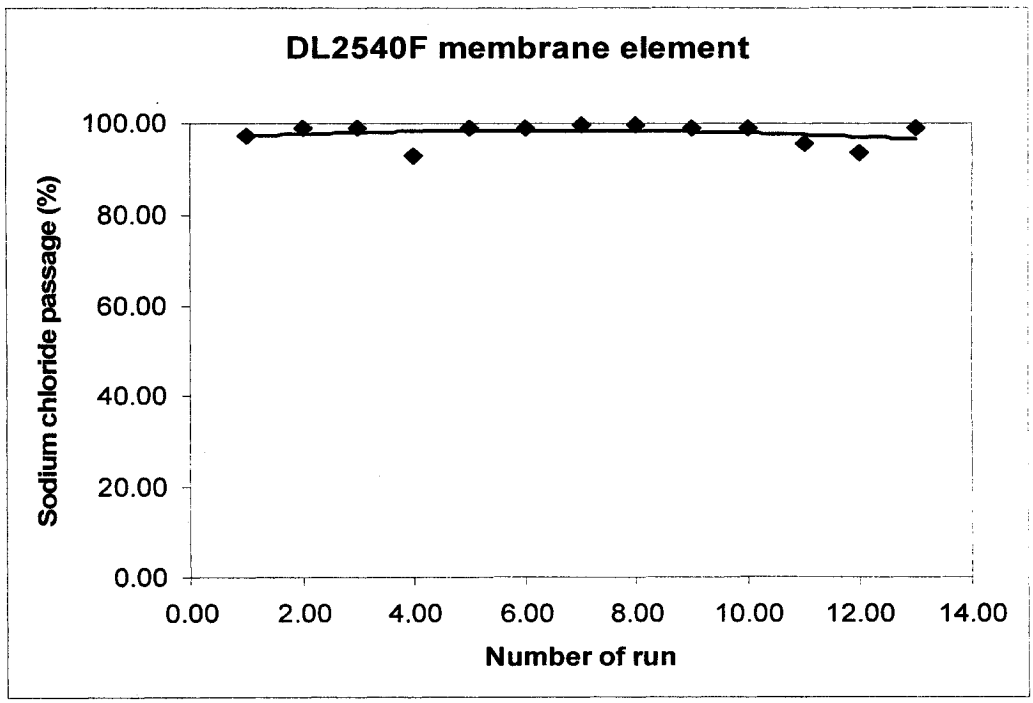

Figure 5-20 Plot of sodium chloride passage vs number of run

Following the similar trend of NF270-2540 membrane element, the DL2540 membrane element showed a decrease in sodium sulfate rejection from 98% in the first run to 74% in the last run as the sodium sulfate in feed increased from 10 g/l in the first runt to 32 g/l in the last run. However, the chloride passage of NF270-2540 membrane possesses almost same high level as NF270-2540 membrane under same feed concentration. Experimental results (Figure 5-20) also showed the passages of sodium chloride for DL2540F membrane were all over 90% for all runs, indicating that the DL2540F membrane element also has good selective ability for sulfate removal of chloralkali brine.

5.2.2.2 Effect of sodium sulfate concentration in feed on permeate flux

Experiments were carried out to study the dependency of permeate flux and sodium sulfate rejection under different sodium sulfate concentration in feed. Figure 5-21 shows the permeate flux under different concentration of Na_2SO_4 at constant pressure (100 psig), temperature (45 °C) and feed flowrate (4 GPM). Permeate flux declined with the increase of sodium sulfate concentration in feed. The results demonstrate that permeate flux declined much faster with increase of sulfate concentration in feed.

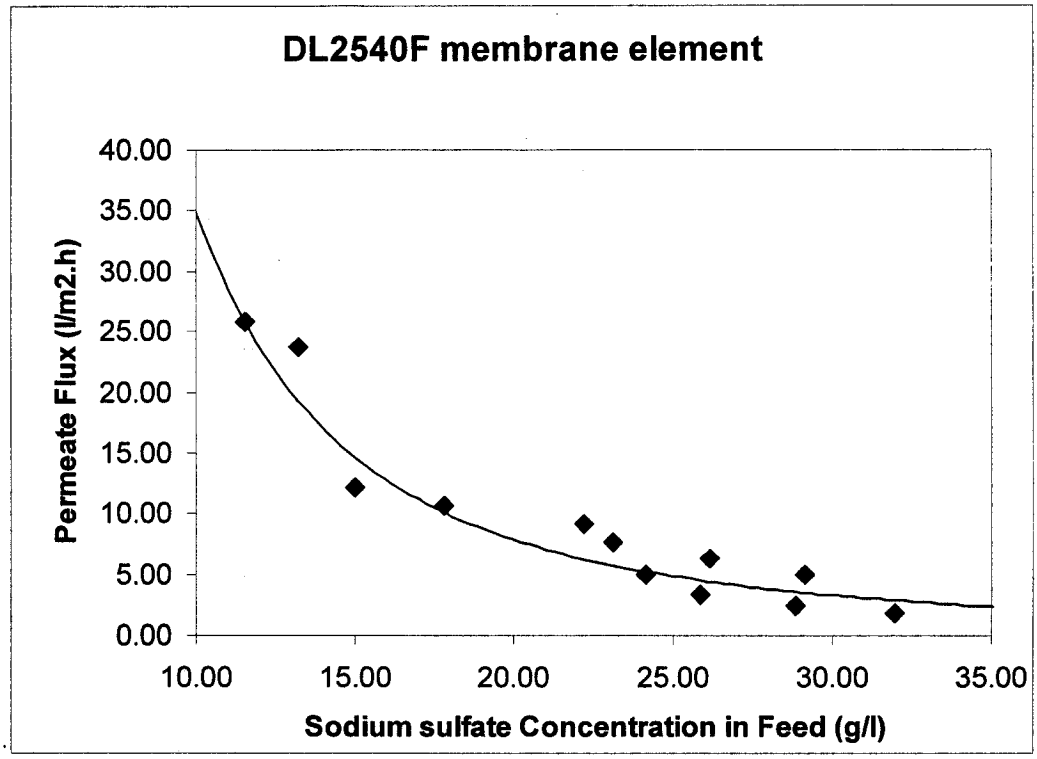

Figure 5-21 Plot of permeate flux vs sodium sulfate concentration in feed

5.2.2.3 Pressure drop of membrane element

Pressure drop along the membrane element was also tested for DL2540F membrane element. As discussed previously, based on hydraulics, the most important parameter affecting the pressure drop is the flow rate of the liquid passing through the membrane module. Similar to NF270-2540 membrane test, the pressure drop increased with the increasing of feed flowrate. Pressure drop vs flow rate were plotted in Figure 5-22 below, the sodium sulfate concentration in feed for these tests were 9.97, 14.99, 22.24, 26.17, 31.93, 36.22 and 39.86 g/l respectively. Similar to the pattern observed with NF270-2540 membrane, the pressure drop increased with the increasing of feed flowrate.

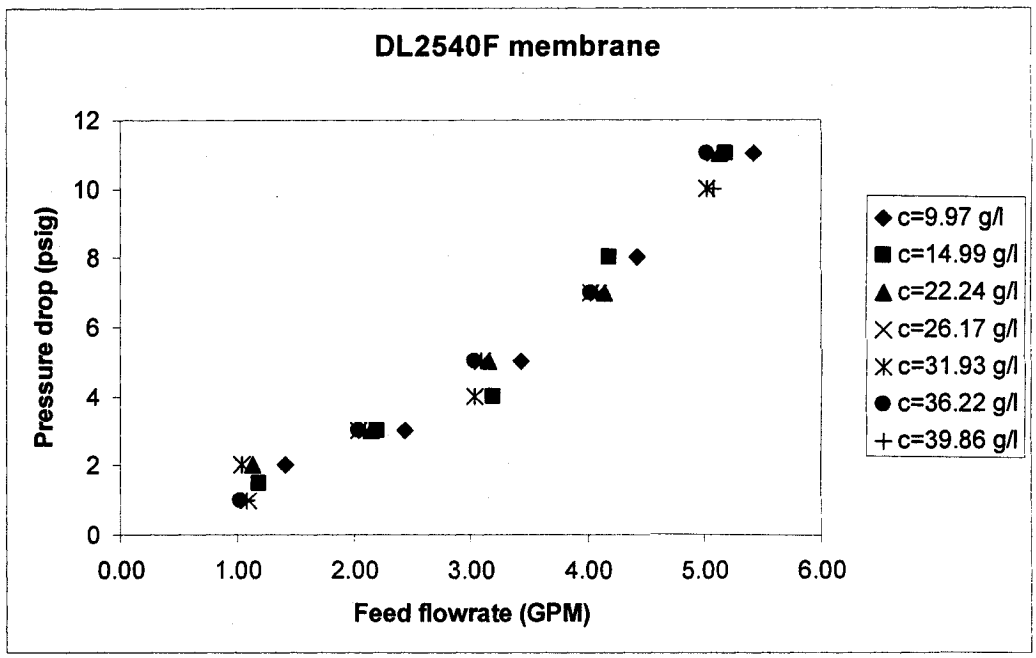

Figure 5-22 Plot of pressure drop vs feed flowrate (1-7 run)

5.2.3 Modeling of nanofiltration membrane processing

5.2.3.1 Theory of concentration polarization

From Equation (2-1), a phenomenological equation has been proposed to characterize the volumetric permeate flux for solution containing one salt species:

$$J_v = L_P(\Delta P - \Delta\pi) \qquad (5\text{-}4)$$

where J_v is the volumetric permeate flux, L_p is the membrane permeability.

Worth mentioning is that in the situation investigated in this study, permeates brine contained around 200 g/L sodium chloride (NaCl) and varied concentration of sodium sulfate (Na_2SO_4). Therefore, the value of L_P not only depends on the membrane properties but also on the brine properties such as viscosity and its ion composition. Interactions between Na^+, Cl^-, and $SO_4^=$ passing through the membrane pores and the charges in individual pores may increase the resistance and lower membrane permeability.

Extension of Equation (5-4) to the chloralkali brine containing primarily NaCl and Na_2SO_4 gives:

$$J_v = L_P\left[(\Delta P - (\Delta\pi_{NaCl} + \Delta\pi_{Na_2SO_4})\right] \quad (5\text{-}5)$$

In the case of sulfate removal from high concentration sodium chloride brines, however, the passage of sodium chloride is high and it is reasonable to assume that $\Delta\pi_{NaCl} = 0$. Therefore, Equation (5-5) is reduced to:

$$J_v = L_P(\Delta P - \Delta\pi_{Na_2SO_4}) \quad (5\text{-}6)$$

The relationship between the osmotic pressure across the membrane ($\Delta\pi_{Na_2SO_4}$) and the sodium sulfate concentration at the membrane interface (C_M^{Na2SO4}) and in the permeate (C_P^{Na2SO4}) is given as follows:

$$\Delta\pi_{Na_2SO_4} = RT(C_M^{Na_2SO_4} - C_P^{Na_2SO_4}) \tag{5-7}$$

where R is the universal gas constant, which has a value of 1.20591 PSI L/mol-K, and T the temperature in Kelvin.

Consider concentration polarization of sodium sulfate on the membrane surface in tangential flow filtration with the assumption of complete NaCl passage, the mass balance on Na_2SO_4 at the membrane interface at steady state gives:

$$J_V = -k \ln\left[\frac{C_M^{Na_2SO_4} - C_P^{Na_2SO_4}}{C_F^{Na_2SO_4} - C_P^{Na_2SO_4}}\right] \tag{5-8}$$

where $C_F^{Na_2SO_4}$ is sodium sulfate concentrations in the feed and k the mass transfer coefficient, which is given by the following equation:

$$k = \frac{D}{\delta} \tag{5-9}$$

where D is the molecular diffusion coefficient of sodium sulfate and σ the thickness of gel layer at the membrane interface caused by concentration polarization of sodium sulfate.

Rearrangement of Equation (5-8) gives:

$$C_M^{Na_2SO_4} = C_P^{Na_2SO_4} + (C_F^{Na_2SO_4} - C_P^{Na_2SO_4}) \exp(\frac{J_v}{k}) \qquad (5\text{-}10)$$

By using Equation (5-10), the sulfate concentration on membrane surface can be calculated.

5.2.3.2 Modeling of concentration polarization

Sodium sulfate concentration at membrane interface and mass transfer coefficient at different feed sulfate concentrations can be calculated by solving Equation (5-7) and (5-10), and fitting Equation (5-6) to experimental data. Calculation results for sulfate concentration on membrane surface (C_m) for DL2540F and NF270-2540 membrane elements are shown in Figure 5-23 and 5-24 as following.

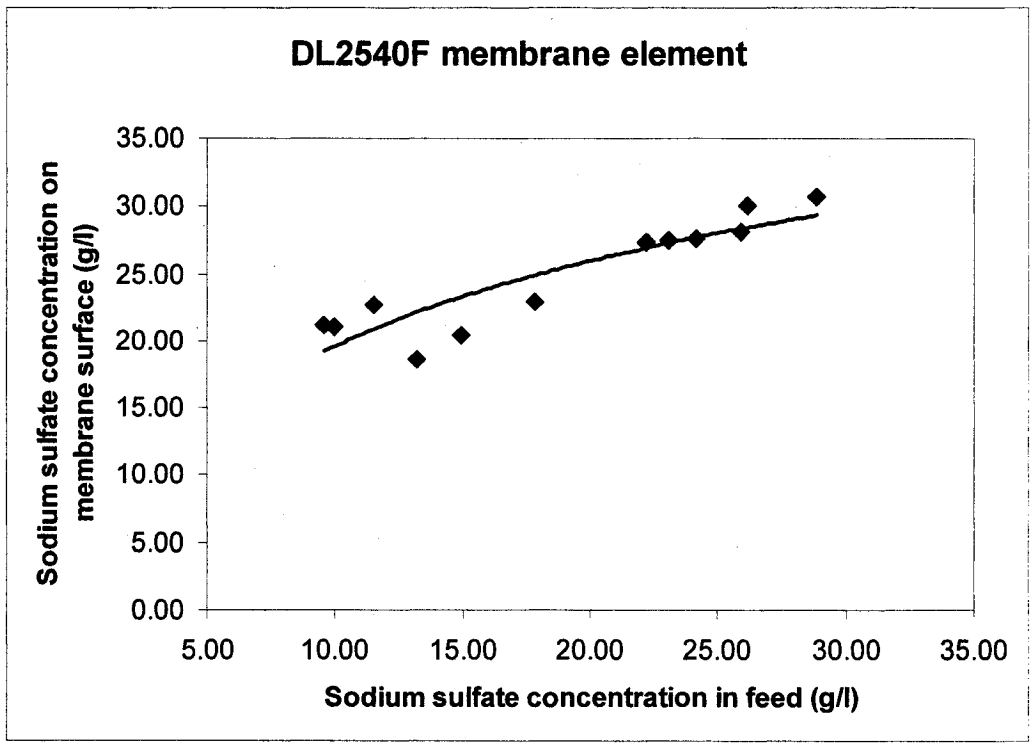

Figure 5-23 Result of calculation of concentration on membrane surface: Effect of feed concentration for DL2540F membrane element at 100 psig, 45 °C

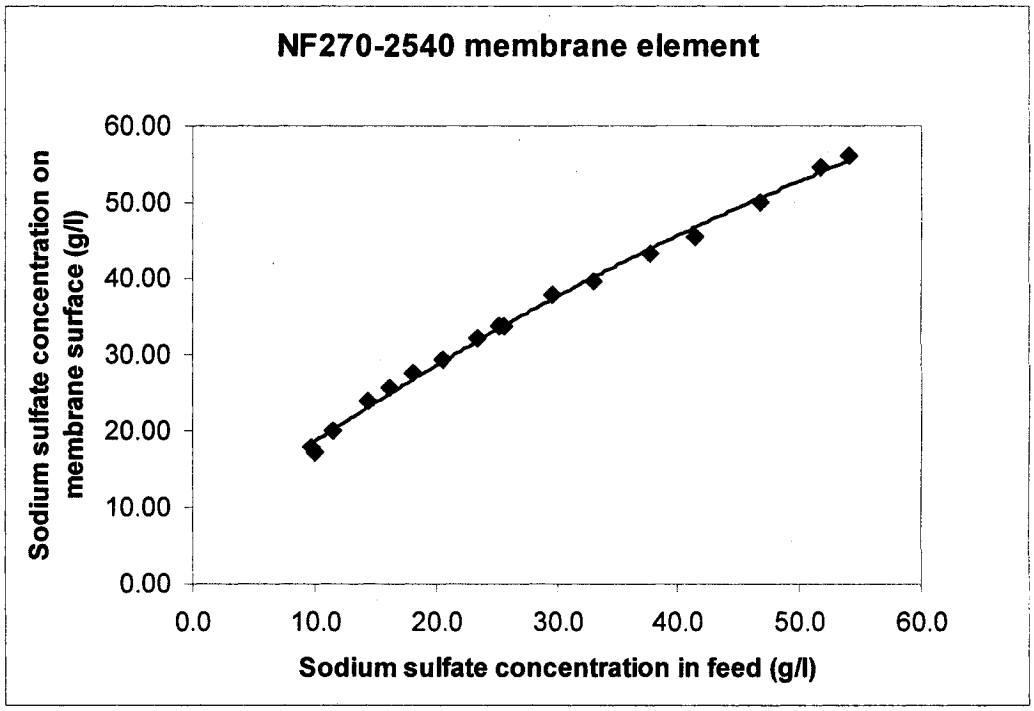

Figure 5-24 Result of calculation of concentration on membrane surface: Effect of feed concentration for NF270-2540 membrane element at 150 psig, 45 °C

As seen in Figures 5-23 and 5-24, for both DL2540F membrane element at 100 PSI and NF270-2540 membrane element at 150 PSI, chloride concentration at membrane interface increased with the increasing of sulfate concentration in feed. These results are reasonable since higher sulfate concentration in feed naturally leads to higher concentration at membrane interface.

The comparison of model calculated permeate flux and experimental permeate flux was plotted in Figure 5-25. This output summary indicates that the model explains the

data quite well. The R Squared value suggests that it explains 93.5% of the variation in the experiments.

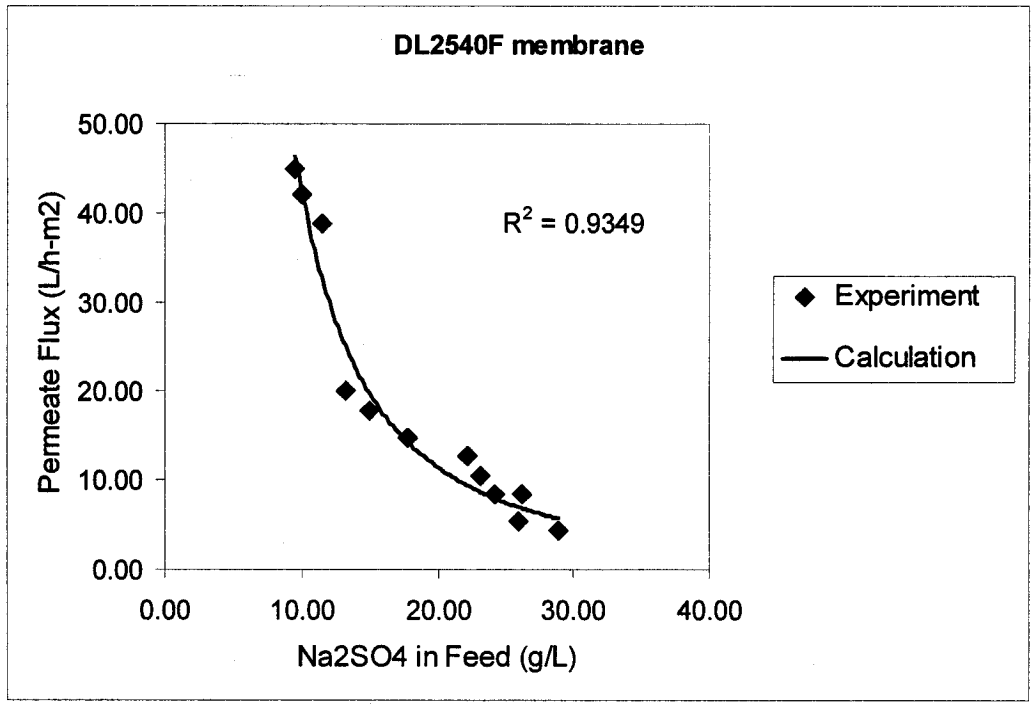

Figure 5-25 Plot of calculation permeate flux vs experimental permeate flux

5.2.3.3 Donnan-Steric partitioning Pore Model (DSPM)

The bulk components consist of Na^+, Cl^- and SO_4^{2-} ions. For ions/solutes to permeate across the membrane, each ion/solute will move from the bulk solution through the film layer, membrane interface and inside the membrane. The proposed model – DSPM model takes into account the transport across all the mentioned mediums.

Concentration polarization close to the membrane surface is assumed to occur within a boundary film layer of thickness, δ, which is dependent on the mass transfer characteristics of the system. For a system containing charged ions, Donnan-Steric partitioning Pore Model (DSPM), which is Equation (2-11), will be applied for a mass balance for film layer yield. The equation can be solved by using the boundary conditions at $x = -\delta$, $c = C_m$ and at $x = 0$, $c = C_{wi}$.

In DSPM model, the overall solution of models based on the extended Nernst-Planck equation Eq. (2-11). The expression for potential gradient can be obtained by using Eq. (2-21). In this case, the ions in solution were Na^+, Cl^-, and SO_4^{2-}, so the potential gradient term can be expressed:

$$\frac{d\psi}{dx} = \frac{\frac{z_{Na}V}{D_{Na,p}}(K_{Na,c}c_{Na} - C_{Na,p}) + \frac{z_{Cl}V}{D_{Cl,p}}(K_{Cl,c}c_{Cl} - C_{Cl,p}) + \frac{z_{SO4}V}{D_{SO4,p}}(K_{SO4,c}c_{SO4} - C_{SO4,p})}{\frac{F}{RT}(z_{Na}^2 c_{Na} + z_{Cl}^2 c_{Cl} + z_{SO4}^2 c_{SO4})} \quad (5\text{-}11)$$

The concentration of ion Na^+, Cl^-, and SO_4^2 can be eliminated from Eq. (5-11) using the electroneutrality conditions within the pore and the permeate solution. By definition

$$z_{Na}c_{Na} + z_{Cl}c_{Cl} + z_{SO4}c_{SO4} + X_D = 0 \quad (5\text{-}12)$$

$$z_{Na}C_{Na,p} + z_{Cl}C_{Cl,p} + z_{SO4}C_{SO4,p} = 0 \quad (5\text{-}13)$$

In this model, it is assumed that the membrane only has the ability to reject sulfate ion, chloride and sodium can pass through the membrane boundary film layer freely. In other words, the chloride concentration in membrane is the same as that in bulk solution. Accordingly, only sulfate ion had concentration polarization phenomena, the concentrations of chloride and sodium on both sides of membrane are same. This assumption is reasonable because it has been showed experimentally that DL2540F and NF270-2540 membranes have high passage to chloride and high rejection rate to sulfate. Based on the feed concentration (200 g/l NaCl + 10 g/l Na_2SO_4), we can get:

$$c_{Na} = C_{Na} = 3489.2 mol/m^3 \quad (5\text{-}14)$$

$$c_{cL} = C_{cL} = 3418.8 mol/m^3 \quad (5\text{-}14)$$

The concentration of ion SO_4^{2-} can be determined using Eq. (2-22), here assume that the activity coefficient in membrane and bulk are same. So Eq. (2-22) becomes

$$\frac{c_{SO4}}{C^0_{SO4}} = \Phi \exp(-\frac{z_{SO4}F}{RT}\Delta\Psi_D) \quad (5\text{-}15)$$

The concentration gradient has been approximated with a one-step central difference method. Thus,

$$\frac{dc_{SO4}}{dx} = \frac{c_{SO4}(x = \Delta x) - c_{SO4}(x = 0)}{\Delta x} \tag{5-16}$$

where x = 0 and x = Δx indicates the membrane surface of permeate and feed sides

The sodium sulfate concentration on membrane feed side had been calculated in selection 5.2.3.2. And the sodium sulfate concentration in permeate had been determined experimentally. The average concentration in membrane is defined as,

$$c_{SO4,avg} = \frac{c_{SO4}(x = \Delta x) + c_{SO4}(x = 0)}{2} \tag{5-17}$$

Using the above equations, the contribution of each transport mechanism can be calculated.

By providing the operating conditions of the system (concentration, pressure, temperature), the model will be able to calculate the permeate concentration and rejection of each ion. The permeate flux will also be calculated based on the osmotic pressure at the membrane wall. Once the input data are provided, the osmotic pressure, $\Delta\pi$, can be calculated based on the bulk concentration. Then the Trans membrane

pressure (TMP) can be determined and the permeate flux, J_v, can be calculated based on pressure driving force with guessed permeability L_p using Equation (5-1) – (5-7). This will be done iteratively until the calculated permeate flux fit the experimental data with least square deviation. Once this optimization was reach, permeability L_p cab be determined (L_p = 0.3995 L/h-m^2-PSI), and the concentration at membrane wall will be calculated (Figure 5-23, Figure 5-24).

Knowing permeate flux J_v, and osmotic pressure $\Delta\pi$, equation (2-11) can be solved to obtain the wall concentrations for each solute C_{wi}. Equation ((2-12) – (2-17) will then be solved for the transport inside the membrane to obtain the permeate concentration C_{pi} for each solute. Again iterative calculations are required until the calculation C_{pi} fit the experimental data with least square deviation to determine C_{pi}. Once C_{pi} is determined, then the rejection R can be calculated. By this way, the membrane characteristics can also be determined. The transport of Na^+, Cl^- and SO_4^{2-} will take place in both the film layer as well as inside the membrane.

5.2.3.4 Modeling results and discussion

As described in above Section 2, the contribution of each transport mechanism in the membrane can be calculated and represented in terms of percentage of the total contribution. The analysis has been carried out for Na_2SO_4 and the solute flux (j_i) for SO_4^{2-} ion has been calculated in total and in its components. The analysis has been carried out by using the method of minimizing the square deviation between

calculated results and experimental data. Also, parameters and membrane characters can be calculated by this way. Parameters used in the modeling are listed in the Table 5-2, and simulation results are illustrated in Figure 5-26.

Table 5-2 Parameter used in modeling

Parameter	Symbol	value	Unit
Permeability	L_P	0.3995	$l/h.m^2.psig$
Steric partition term	Φ	0.00029112	dimensionless
Hindered diffusivity	$D_{i,p}$	1.8027×10^{-10}	m^2s^{-1}
Donnan potential difference	$\Delta\Psi_D$	3×10^{-11}	V
Hindrance factor for convection	$K_{i,c}$	0.9995	dimensionless
Faraday constant	F	96500	$C\ mol^{-1}$
Effective membrane charge	X_D	200	mV

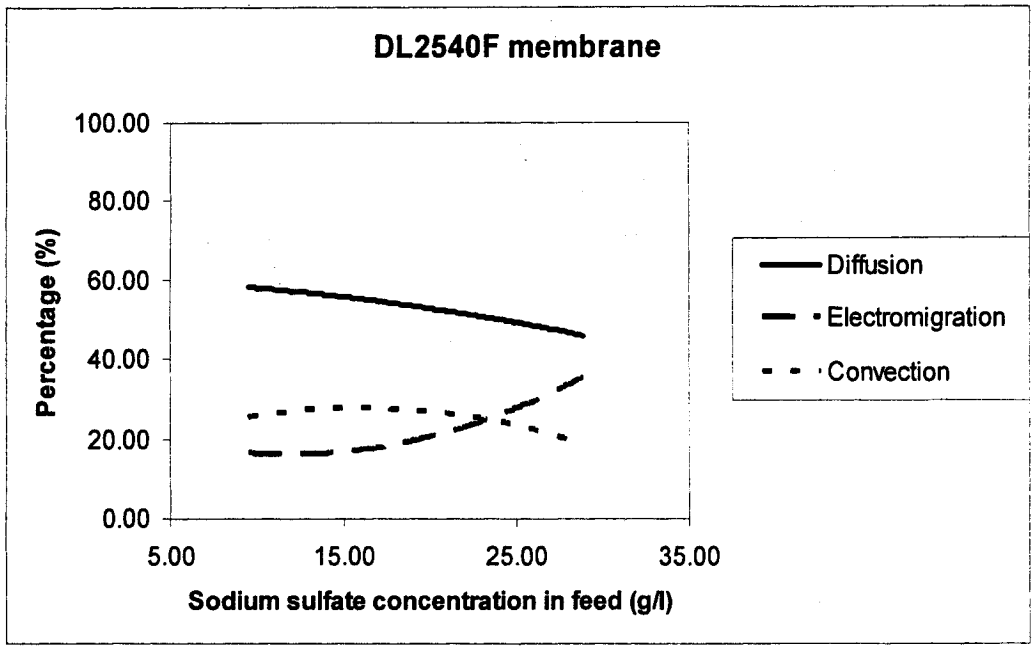

Figure 5-26 Result of the analysis of transport mechanisms: Effect of variation of feed concentration for DL2540F membrane

Figure 5-26 shows the analysis of contribution of three transport mechanisms (diffusion, electromigration and convection) in percentage for DL2540F membrane. It can be seen that all three mechanisms play significant role in mass transport through membrane. The contribution of diffusion decreased from 60.66% - 42.84% with the increase of feed concentration at tested sulfate concentration range from 10 to 30 g/l. The contribution of electromigration increased with the increase of feed concentration from 13.9% at feed concentration of 10 g/l to 38.58% at feed concentration of 30 g/l (Na_2SO_4). Finally, the contribution of convection increased from 23% to 32% with the feed concentration increased from 10 g/l to 14 g/l, then decreased from 32% to 18.5% with the feed concentration increased from 14% to 30%.

The analysis of the transport model for the range of feed concentration tested shows that chloralkali brine which initially contains 200g/l sodium chloride and 10g/l sodium sulfate, all the three transport mechanisms (diffusion, electromigration and convection) play a significant role in the tested range of sulfate concentration. At low sulfate concentration around 10g/l sulfate, convection play major role in mass transport. When feed concentration increase, permeate flux decreased, the contribution of convection decreased. At high feed concentration, the role of electromigration and diffusion contribution for transport mechanisms is high than that in low feed concentration in the determining the rejection of sulfate.

Overall, the model described in the present article is a powerful tool for the characterization of NF membranes and subsequent prediction of separation performance due to the removal of the need for complex nonlinear numerical methods through the reduction of the governing equations to a system of algebraic expressions. In addition, linearization reduces the calculation time required to generate predictions for the rejection of multicomponent solutions.

6. Conclusions

This study investigated the effects of temperature, pressure and sodium sulfate concentration in feed using three commercial membrane elements. Experiments were carried out with a pilot 2.5 inch diameter membrane element system. The results provided valuable guidelines for the design and operation of industrial sulfate removal system for chloralkali industry.

6.1 Performance of different commercial membranes

Experimental results indicate that two commercial nanofiltration membranes, DL2540F by GE Osmonics and NF270-2540 by FilmTec (DOW), are applicable for sulfate removal from concentrated sodium chloride brines similar to that typically encountered in chloralkali industry. DL2540F membrane has better performance in term of sulfate selectivity and water permeability. XN45-2540 membrane element is not suitable for this application.

6.2 Effect of temperature

Temperature was found to no have significant effect on sulfate rejection and chloride passage under the tested condition. However, It was found to have significant

influence on permeate flux. The effects of temperature on flux followed the Arrhenius model. At the same operating condition, DL2540F has the highest permeate flux among these three membrane elements.

6.3 Effect of operating pressure

Tests were carried out using DL2540F, NF270-2540 and XN45-2540 membrane elements. Operating pressure was also found to have no significant effect to sulfate rejection and chloride passage. On the other hand, it was found that the permeate flux increased linearly with the operating pressure when the feed contained 200 g/L and 10 g/L, which was compatible with the fact that transmembrane pressure is the driving force for a NF process.

6.4 Effect of feed concentration

Sodium concentration in feed had significant effects on permeate flux, sulfate rejection, and sulfate concentration at membrane interface and in permeate. Sulfate rejection and permeate flux reduced sharply with the increase of sulfate concentration in feed.

6.5 Simulation of transport mechanism

Theoretical simulation results confirmed the similar pattern as experimental data. And the analysis of the transport model in the range of feed concentration tested shows that generally the contribution of each transport mechanism in the (diffusion, electromigration and convection) play different role for this particular project under different feed concentration, and the variation of these three transport mechanism can be predicted by DSPM model. With the increase of feed concentration, the contribution of diffusion, the contribution of electromigration increase, and the contribution of convection decrease.

7. Recommendation

Based on the results of the research, a recommendation can be provided for sulfate removal from concentrated sodium chloride brines of chloralkali industry:

DL serials commercial nanofiltration membrane elements manufactured by GE Osmonics, are most suitable for the treatment of chloralkali brine.

Further work should include the study of membrane performance under higher operating pressure and higher feed concentration. The performance of industrial scale membrane application also needs to be investigated and documented.

References

1. D. Bessarabov, Z. Twardowski, Industrial application of nanofiltration – new perspectives, *Membrane Technology*, Sep. 2002
2. J. Wagner, Membrane Filtration Handbook, 2nd edition, Osmonics Inc, Nov, 2001
3. R. Rautenbach, A. Groschl, Separation Potential of Nanofiltration Membranes, *Desalination*, 77 (1990) 73-84
4. W.B. Samuel de Lint, Nieck E. Benes, J. Lyklema etc., (2003), Ion Adsorption Parameters Determined from Zeta Potential and Titration Data for a γ-Alumina Nanofiltration Membrane, *Langmuir*, 19, 14
5. H.C. van der Horst, J.M.K. Timmer, T. Robbertson, J. Leenders, Use of nanofiltration for concentration and demineralization in the dairy industry: model for mass transport, *J. Membr. Sci.* 104 (1995) 205-218
6. H.S. Alkhatim, M.I. Alcaina, E. Soriano, M.I. Iborra, J. Lora, J. Arnal, Treatment of whey effluents from dairy industries by nanofiltration membranes, *Desalination* 119 (1998) 177-184
7. R. P. Lakshminarayan, M. Cheryan, N. Rajagopalan, Consider nanofiltration for membrane separations, *Chem. Eng.* Prog. 90 (1994) 68-74
8. E. Vellenga, G. Tragardh, Nanofiltration of combined salt and sugar solutions: coupling between retentions, *Desalination* 120 (1998) 211-220
9. J. Durham, J. A. Hourigan, R.W. Sleigh, R.L. Johnson, Process for recycling of nutrients from food process streams, PCT WO9904903, 1999

10. M. Schmidt, D. Paul, K.-V. Peinemann, S. Kattanek, H. Roedicker, Nanofiltration of process solutions highly contaminated with low-molecular organic compounds, F&S Filtr. Sep. 10 (1996) 245-251

11. J. Fritsch, B. Zimmermann, Recycling of caustic cleaning solution with nanofiltration, *F&S Filtr. Sep.* 12 (1998) 248-253

12. S. McGrath, The talosave brine recovery process for treatment of ion exchange regenerant in sugar refineries, Publ. Tech. Pap. Proc. Annual Meet. Sugar Ind. Technol. 57 (1998) 299-309

13. S. Cartier, M.A. Theoleyre, M. Decloux, Treatment of sugar decolorizing resin regeneration waste using nanofiltration, *Desalination* 113 (1997) 7-17

14. G. Cueille, V. Thoraval, A. Byers, S. McGrath, D. Segal, R. Kahn, Industrial waste brine treatment in the cane sugar refining process, *Filtr. Sep.* 34 (1997) 25-27

15. S. Wadley, C.J. Brouckaert, L.A.D. Baddock, C.A. Buckley, Modeling of nanofiltration applied to the recovery of salt from waste brine at a sugar decolorization plant, *J. Membr. Sci.* 102 (1995) 163-75

16. A. Srivastava, A.N. Pathak, Modern technologies for distillery effluent treatment, *J. Sci. Ind. Res.* 57 (1998) 388-392

17. J.M.K. Timmer, H.C. van der Horst, T. Robbertsen, Transport of lactic acid through reverse osmosis and nanofiltration membranes, *J. Membr. Sci.* 85 (1993) 205-216

18. J.M.K. Timmer, J. Kromkamp, T. Robbertsen, Lactic acid separation from fermentation broths by reverse osmosis and nanofiltration, *J. Membr. Sci.* 92 (1994) 185-197

19. I.S. Han, M. Cheryan, Nanofiltration of model acetate solutions, *J. Membr. Sci.* 107 (1995) 107-113

20. J.M.K. Timmer, M.P.J. Speelmans, H.C. van der Horst, Separation of amino acids by nanofiltration and ultrafiltration membranes, *Sep. Purif. Technol.* 14 (1998) 133-144

21. T. Schaefer, R. Gross, J. Janitza, J. Trauter, Nanofiltration of dye wastewater, *F&S Filtr. Sep.* 13 (1999) 9-16

22. J. Sojka-Ledakowicz, T. Koprowski, W.Machnowski, H. H. Knudsen, Membrane filtration of textile dyehouse wastewater for technological water reuse, *Desalination* 119 (1998) 1-10

23. R.W. Bowen, W.A. Mohammad, A theoretical basis for specifying nanofiltration membranes - dye/salt/water streams, *Desalination* 117 (1998) 257-264

24. J.P. van 't Hul, I.G. Racz, T. Reith, The application of membrane technology for reuse of process water and minimization of waste water in a textile washing range, *J. Soc. Dyers Colour.* 113 (1997) 287-294

25. A. Cassano, E. Drioli, R. Molinari, Recovery and reuse of chemicals in unhairing, degreasing and chromium tanning processes by membranes, *Desalination* 113 (1997) 251-261

26. A. Cassano, E. Drioli, R. Molinari, C. Bertolutti, Quality improvement of recycled chromium in the tanning operation by membrane processes, *Desalination* 108 (1997) 193-203

27. K.-H. Ahn, H.-Y. Cha, I.-T. Yeom, K.-G. Song, Application of nanofiltration for recycling of paper regeneration wastewater and characterization of filtration resistance, *Desalination* 119 (1998) 169-176

28. M. Manttari, J. Nuortila-Jokinen, M. Nystrom, Influence of filtration conditions on the performance of NF membranes in the filtration of paper mill total effluent, *J. Membr. Sci.* 137 (1997) 187-199

29. M. D. Afonso, M. Norberta De Pinho, Nanofiltration of bleaching pulp and paper effluents in tubular polymeric membranes, *Sep. Sci. Technol.* 32 (1997) 2641-2658

30. V. Geraldes, M. Norberta de Pinho, Process water recovery from pulp bleaching effluents by an NF/ED hybrid process, *J. Membr. Sci.* 102 (1995) 209-21

31. M. J. Rosa, M. Norberta de Pinho, The role of ultrafiltration and nanofiltration on the minimisation of the environmental impact of bleached pulp effluents, *J. Membr. Sci.* 102 (1995) 155-61

32. Z. Twardowski, J.G. Ulan, Nanofiltration of concentrated aqueous salt solutions, US 5858240, 1995

33. M.-B. Hagg, Membranes in chemical processing. A review of applications and novel developments, Sep. Purif. Methods 27 (1998) 51-168

34. K. Maycock, Z. Twardowski, J. Ulan, A new method to remove sodium sulfate from brine, Mod. *Chlor-Alkali Technol.* 7 (1998) 214-221

35. H.J.F.A. Hesse, M.J. Smit, F.J. Du Toit, A method for removal of carbon dioxide from a process gas, PCT WO 9825688, 1998

36. K.F. Lin, Bromide separation and concentration using semipermeable membranes, US 5158683, 1998

37. R.S. Danziger, Purification of liquids contaminated by filamentary molecules, PCT WO 9723279, 1997

38. A. Hoffmann, R. Kummel, J. Tschernjaew, P.M. Weinspach, Generation of supersaturations in nanofiltration. Determination of dimensioning data for a new crystallization process, Chem.-Ing.-Tech. 69 (1997) 831-833

39. P.K. Eriksson, L.A. Lien, D.H. Green, Membrane technology for treatment of wastes containing dissolved metals, Extr. Process. Treat. Minimization Wastes 1996, Proc. 2nd Int. Symp. (1996) 649

40. M. Kyburz, Acid preparation by reverse osmosis and nanofiltration, *F&S Filtr. Sep.* (1995) 13-20

41. S. Barfknecht, Method and device for separation of metal ions from contaminated wash water, Ger. Offen. DE 19729493, 1999

42. J. Hammer, A. Richter, W. Kraus, Method and device for treating wastewaters from a chemicalmechanical polishing process in chip manufacturing, PCT WO 9849102, 1998

43. P. Katselnik, S.Y. Morcos, Reduction of nickel in plating operation effluent with nanofiltration, Plat. Surf. Finish. 85 (1998) 46-47

44. P. Katselnik, S.Y. Morcos, Reduction of nickel in plating operation effluent with nanofiltration, *Plat. Surf. Finish.* 85 (1998) 46-47

45. D.H. Green, Column-treatment system with nanofiltration stage for removal of metal ions after acidic leaching of copper ores, US 5476591, 1995

46. D.H. Green, Copper recovery from lixivant solutions in ore leaching, PCT WO 9530471, 1995

47. B. Abolmaali, I. Yassine, P. Capone, Water recovery from an aluminum can manufacturing process using spiral wound membrane elements, Proc. - WEFTEC '96, Annu. Conf. Expo., 69th 5 (1996) 407-412

48. K.-W. Mok, P.J. Pickering, J.E.V. Broome, Method and apparatus for recovery and purification of lithium from lithium battery waste, PCT WO 9859385, 1998

49. H. Matamoros, C. Cabassud, Y. Aurelle, Nanofiltration processes for cutting oil wastewater treatment, Proc. – 7th World Filtr. Congr., 2 (1996) 531-535

50. M.R. Adiga, Treatment of plating wastewater for removal of metals, Can. Pat. Appl. CA 2197525, 1997

51. P.K. Eriksson, L.A. Lien, D.H. Green, Membrane technology for treatment of wastes containing dissolved metals, Proc. 2nd Int. Symp. (1996) 649-658

52. C. Jönsson, A.-S. Jönsson, The influence of degreasing agents used at car washes on the performance of ultrafiltration membranes, *Desalination* 100 (1996) 115-123

53. C. Visvanathan, B.D. Marsono, B. Basu, Removal of THMP by nanofiltration: effects of interference parameters, *Water Res.* 32 (1998) 3527-3538

54. J. Schaep, B. Van der Bruggen, S. Uytterhoeven, R. Croux, C. Vandecasteele, D. Wilms, E. Van Houtte, F. Vanlerberghe, Removal of hardness from groundwater by nanofiltration, *Desalination* 119 (1998) 295-302

55. E. Wittmann, P. Cote, C. Medici, J. Leech, A.G. Turner, Treatment of a hard borehole water containing low levels of pesticide by nanofiltration, *Desalination* 119 (1998) 347-352

56. N.A. Braghetta, F. DiGiano, W.P. Ball, OM accumulation at NF membrane surface: impact of chemistry and shear, *J. Environ. Eng.* 124 (1998) 1087-1098

57. A.I. Schafer, A.G. Fane, T.D. Waite, Nanofiltration of natural organic matter: removal, fouling and the influence of multivalent ions, *Desalination* 118 (1998) 109-122

58. M. Alborzfar, G. Jonsson, C. Gron, Removal of natural organic matter from two types of humic ground waters by nanofiltration, *Water Res.* 32 (1998) 2983-2994

59. S.-H. Yoon, C.-H. Lee, K.-J. Kim, A.G. Fane, Effect of calcium ion on the fouling of nanofilter by humic acid in drinking water production, *Water Res.* 32 (1998) 2180-2186

60. B. van der Bruggen, J. Schaep, W. Maes, D. Wilms, C. Vandecasteele, Nanofiltration as a treatment method for the removal of pesticides from ground waters, *Desalination* 117 (1998) 139-147

61. S.-S. Chen, J.S. Taylor, C.D. Norris, J.A.M.H. Hofman, Flat sheet testing for pesticide removal by varying RO/NF membrane, Membr. Technol. Conf. Proc. (1997) 843-855

62. R. Hopman, J.P. van ver Hoek, J.A.M. van Paassen, J.C. Kruithof, The impact of NOM presence on pesticide removal by adsorption: problems and solutions, Water Supply 16 (1/2, 21st International Water Services Congress and Exhibition, 1997) (1998) 497-501

63. P. Brandhuber, G. Amy, Alternative methods for membrane filtration of arsenic from drinking water, *Desalination* 117 (1998) 1-10

64. T. Urase, J.-I. Ohb, K. Yamamoto, Effect of pH on rejection of different species of arsenic by nanofiltration, *Desalination* 117 (1998) 11-18

65. P. Bryant, J. Basta, Process for treating wastewater, PCT WO 9839258, 1998

66. L. Durand-Bourlier, J.-M. Laine, Use of NF and EDR technology for specific ion removal: fluoride, Proc. Membr. Technol. Conf. (1997) 1-16

67. P. Natarajan, State-of-the-art techniques in reverse osmosis, nanofiltration and electrodialysis in drinking-water supply, Water Supply 14 (3/4, 20th International Water Supply Congress and Exhibition, 1995) (1996) 308-310

68. M. Muntisov, P. Trimboli, Removal of algal toxins using membrane technology, *Water* 23 (1996) 34

69. H.S. Vrouwenvelder, J.A.M. van Paassen, H.C. Folmer, JA.M.H. Hofman, M.M. Nederlof, D. van der Kooij, Biofouling of membranes for drinking water production, *Desalination* 118 (1998) 157-166

70. P. Henigin, U. Eymann, Method for treatment of landfill leachate, Ger. Offen. DE 19728414, 1997

71. T.A. Peters, Purification of landfill leachate with reverse osmosis and nanofiltration, *Desalination* 119 (1998) 289-293

72. W. Heine, J. Mohn, Membrane separation of liquid mixtures such as landfill leachate, Ger. Offen. DE 19702062, 1998

73. J.P. Maleriat, D. Trebouet, P. Jaouen, F. Quemeneur, Study of a combined process using natural flocculating agents and crossflow filtration for the processing of an aged landfill leachate, Proc. 7th World Filtr. Congr. 2 (1996) 507-511

74. E. Wichterey, D. Klos, Treatment of wastewaters containing inorganic and organic pollutants, Ger. Offen. DE 19605580, 1996

75. J.L. Bersillon, P. Cote, State-of-the-art techniques in reverse osmosis, nanofiltration and electrodialysis in drinking-water supply, Water Supply 14

(3/4, 20th International Water Supply Congress and Exhibition, 1995) (1996) 304-306

76. K. Linde, A.-S. Jönsson, Nanofiltration of salt solutions and landfill leachate, *Desalination* 103 (1995) 223-32

77. Y.K. Kharaka, G. Ambats, T. Presser, R. A. Davis, Removal of selenium from contaminated agricultural drainage water by nanofiltration membranes, *Appl. Geochem.* 11 (1996) 797-802

78. M.K. Turner, Effective Industrial Membrane Processes: Benefits and Opportunities, Elsevier Applied Science, 1991

79. Mark C. Porter, Handbook of Industrial Membrane Technology, Notes Publications, 1990

80. D. Barba, F. Evangelista, H. Wang, D. Spera, The effects of osmotic pressure and fouling during a concentration process of BSA solutions by ultrafiltration, *Desalination*, 144 (1997) 183-188

81. Moore, W. J. Physical Chemistry, 2nd ed.; Prentice Hall: Englewood Cliffs, NJ, 1955; Chapters 6 and 15.

82. A.A. Zavitsas, Properties of water solutions of electrolytes and nonelectrolytes, *J. Phys. Chem.* B 2001, 105, 7805-7817

83. Y.H. Su, S.B. Riffat, A thermodynamic approach to calculating the operating osmotic pressure of pressure-driven membrane separation absorption cycles, *International J. of Thermal Sci.*, 43 (2004) 1197-1201

84. L. P. Raman, (1994) Consider Nanofiltration for Membrane Separations, *Chemical Engineering Process*, March 1994

85. W. R Bowen, A. W. Mohammad, Characterization and prediction of Nanofiltration Membrane Performance — A General Assessment, *Trans IChemE*, Vol 76, Part A, Nov 1998

86. W. R. Bowen, A.W. Mohammad and N. Hilal, 1997,Characterisation of nanofiltration membranes for predictive purposes use of salts, uncharged solutes and atomic force microscopy, *J. Membrane Sci*, 126: 91-105.

87. W.R. Bowen and A.W. Mohammad (1998), Diafiltration by nanofiltration: prediction and optimization, *AIChE J* 44: 1719-1812.

88. A. Mohammad, M. Takriff, Predicting flux and rejection of multicomponent salts mixture in nanofiltration membranes, *Desalination*, 157 (2003) 105-111

89. K. Kosutic, I. Novak, L. Sipos, B. Kunst, Removal of sulfates and other inorganics from potable water by nanofiltration membranes of characterized porosity, *Separation and Purification Technology*, 37 (2004) 177-185

90. T. Tsuru, S. Nakao, S. Kimura, Calculation of ion rejection by extended Nernst-Planck equation with charged reverse osmosis membranes for single and mixed electrolyte solutions, *J. Chem. Eng. of Japan* 24 (1991) 511-517

91. X.L.Wang, T. Tsuru, S. Nakao, S. Kimura, Electrolyte transport through nanofiltration membranes by the space charge model and the comparison with the Teorell Meyer Sievers model, *J. Membr. Sci.* 103 (1995) 117-133

92. Petersen, R.J. (1993) Composite reverse osmosis andnanofiltration membranes, *J. Membr. Sci.*, 83 81

93. Richard W. Baker, Membrane Technology and Applications, McGraw-Hill, 2000

94. T. Matsuura, Progress in membrane science and technology for seawater desalination – a review, *Desalination* 134 (2001) 47-54

95. Dresner, L. (1972). Some remarks on the integration of extended Nernst–Planck equation in the hyperfiltration of ulticomponent solutions. *Desalination*, 10, 27–46.

96. W. Bowen, J. Welfood, and P. Williams, Linearized Transport Model for Nanofiltration: Development and Assessment, AJChE Journal, April 2002, Vol. 48, No. 4

97. A. Mohammad, M. Takriff, Predicting flux and rejection of multicomponent salts mixture in nanofiltration membranes, *Desalination*, 157 (2003) 105-111

98. H. Peng, The Treatment of Bilge Water using a MF/UF Hybrid Membrane System: Membrane Fouling, Cleaning and The Effect of Constituents on Flux Decline, M.A.S thesis, Department of Chemical Engineering, University of Ottawa, 2002

Appendices

Appendix A – FilmTec NF270-2540 Nanofiltration Membrane Test

Date: April 1, 2004 Thursday

Membrane Type: FilmTec NF270-2540 Nanofiltration Membrane Element

Pressure: 100 Psig Feed Flowrate: 2 GPM

Temperature: 25 °C

Table A-1 Sulfate Rejection Test of NF270-2540

Sample #	Sulfate rejection (%)	Pressure (psig)	Feed flowrate (GMP)	Temperature (°C)
1	94.60	50	1	25
2	95.29	50	1	30
3	96.18	50	1	39
4	96.71	50	4	40
5	97.70	50	4	40
6	97.30	100	1	40
7	97.53	100	4	40
8	97.99	100	4	40
9	98.22	150	4	30
10	97.40	150	4	35
11	97.89	150	4	40
12	98.32	150	4	45
13	98.26	150	1	45

Table A-2 Chloride Passage Test of NF 270-2540 membrane element

Sample #	Chloride Passage (%)	Pressure (psig)	Feed flowrate (GMP)	Temperature (°C)
1	92.71	50	1	25
2	92.46	50	1	30
3	93.73	50	1	40
4	92.63	50	4	40
5	96.75	50	4	40
6	88.08	100	1	40
7	98.34	100	4	40
8	97.16	100	4	40
9	98.00	150	4	30
10	96.79	150	4	35
11	98.23	150	4	40
12	99.69	150	4	45
13	91.19	150	1	45

Table A-3 Permeate Flux Test of NF260-2540 Membrane Element

Volume (ml)	Time (s)	Permeate (ml/s)	Average Permeate (ml/s)	Pressure (PSI)	Feed Flowrate (GPM)	Temperature ©
44.00	12.47	3.53				
40.80	11.00	3.71	3.57	50	1	25
38.70	10.60	3.65				
45.90	13.60	3.38				
32.00	13.16	2.43				
38.50	15.60	2.47	2.47	50	1	30
43.80	17.37	2.52				
39.80	13.25	3.00				
41.00	12.13	3.38	3.22	50	1	40
42.50	12.94	3.28				
41.00	12.78	3.21				
43.50	13.25	3.28	3.26	50	4	40
47.00	14.31	3.28				
40.50	12.62	3.21	3.19	50	4	40
42.70	13.43	3.18				
39.00	3.68	10.60				
47.30	4.60	10.28	10.25	100	1	40
47.50	4.81	9.88				
47.10	4.56	10.33				
45.50	4.34	10.48	10.38	100	4	40
47.50	4.60	10.33				
47.70	4.69	10.17				
47.80	4.75	10.06	10.09	100	4	40
49.30	4.91	10.04				
44.80	3.60	12.44				
48.00	3.65	13.15	12.85	150	4	30
47.00	3.63	12.95				
45.00	2.72	16.54				
46.50	3.06	15.20	15.33	150	4	35
49.00	3.44	14.24				
48.50	2.72	17.83				
46.70	2.72	17.17				
46.00	2.95	15.59	16.95	150	4	40
42.00	2.62	16.03				
49.90	2.75	18.15				
44.60	2.15	20.74				
44.20	2.16	20.46	20.65	150	1	45
41.50	2.00	20.75				

Date: April 12, 2004

Membrane Type: FilmTec NF270-2540 Nanofiltration Membrane Element

Pressure: 100 Psig Feed Flowrate: 2 GPM

Sodium sulfate concentration in feed (g/l): 8.98

Table A-4 Sulfate Rejection Test of NF 270-2540 membrane element

Sample #	Sulfate Rejection (%)	Pressure (psig)	Feed flowrate (GMP)	Temperature (°C)
1	92.16	100	2	25
2	92.20	100	2	30
3	91.15	100	2	35
4	91.48	100	2	40
5	90.08	100	2	45

Table A-5 Chloride Passage Test of NF 270-2540 membrane element

Sample #	Chloride Passage (%)	Pressure (psig)	Feed flowrate (GMP)	Temperature (°C)
1	97.60	100	2	25
2	91.04	100	2	30
3	89.42	100	2	35
4	82.15	100	2	40
5	85.40	100	2	45

Table A-6 Permeate Flux Test of NF270-2540 Membrane Element

Sample #	Volume (ml)	Time (s)	Permeate (ml/s)	Average Permeate (ml/s)	Permeate Flux ($l/h.m^2$)
1	47.5	7.34	6.47	6.50	6.4
	46.0	7.04	6.53		6.5
	47.0	7.16	6.56		6.5
2	45.8	6.13	7.47	7.51	7.4
	44.9	6.00	7.48		7.5
	48.0	6.28	7.64		7.6
3	44.8	4.78	9.37	9.46	9.3
	45.9	4.85	9.46		9.4
	47.5	4.93	9.63		9.6
4	48.5	4.50	10.78	10.61	10.7
	48.0	4.60	10.43		10.4
	47.3	4.41	10.73		10.7
5	47.5	3.87	12.27	12.56	12.2
	48.0	3.81	12.60		12.6
	45.3	3.50	12.94		12.9

Appendix B – GE DL2540F Nanofiltration Membrane Test

Date: April 21, 2004 Wednesday

Membrane Type: GE DL2540F Nanofiltration Membrane Element

Pressure: 50 Psig Feed Flowrate: 2 GPM

Sodium sulfate concentration in feed (g/l): 8.98 g/l

Table B-1 Sulfate Rejection Test of DL2540F membrane element

Sample #	Sulfate rejection (%)	Pressure (psig)	Feed flowrate (GMP)	Temperature (°C)
1	98.32	50	2	25
2	99.54	50	2	30
3	99.03	50	2	35
4	99.37	50	2	40
5	99.96	50	2	45
6	98.95	100	2	25
7	98.99	100	2	30
8	99.96	100	2	35
9	99.79	100	2	40
10	99.66	100	2	45

Table B-2 Chloride Passage Test of DL 2540F membrane element

Sample #	Chloride Passage (%)	Pressure (psig)	Feed flowrate (GMP)	Temperature (°C)
1	92.51	50	2	25
2	87.60	50	2	30
3	90.93	50	2	35
4	90.66	50	2	40
5	87.10	50	2	45
6	99.81	100	2	25
7	98.30	100	2	30
8	93.85	100	2	35
9	91.23	100	2	40
10	99.66	100	2	45

Table B-3 Permeate Flux Test of DL 2540F membrane element

Permeate Volume (ml)	Time (s)	Permeate (ml/s)	Average Permeate (ml/s)	Temperature °C	Pressure (psig)	Flowrate (GPM)
46.80	12.09	3.87				
46.00	12.00	3.83	3.84	25	50	2
46.00	12.03	3.82				
47.50	11.09	4.28				
46.30	10.56	4.38	4.35	30	50	2
46.30	10.56	4.38				
46.00	9.28	4.96				
45.80	9.13	5.02	5.02	35	50	2
47.30	9.31	5.08				
45.20	8.06	5.61				
46.20	8.09	5.71	5.69	40	50	2
46.50	8.10	5.74				
47.50	7.37	6.45				
47.10	7.35	6.41	6.43	45	50	2
47.10	7.32	6.43				
48.50	4.46	10.87				
48.20	4.40	10.95	10.88	25	100	2
48.70	4.50	10.82				
48.70	4.00	12.18				
48.90	3.84	12.73	12.56	30	100	2
48.70	3.81	12.78				
49.00	3.47	14.12				
49.50	3.45	14.35	14.15	35	100	2
49.50	3.54	13.98				
48.20	3.07	15.70				
48.00	3.00	16.00	16.04	40	100	2
50.00	3.10	16.13				
49.50	3.03	16.34				
49.50	2.78	17.81				
50.00	2.81	17.79	17.78	45	100	2
50.00	2.82	17.73				

Date: April 26, 2004 Monday

Membrane Type: GE DL2540F Nanofiltration Membrane Element

Temperature: 30 and 45 °C Feed Flowrate: 2 GPM

Sodium sulfate concentration in feed: 8.56 g/l

Sodium chloride concentration in feed: 168.87 g/l

Table B-4 Sulfate Rejection Test of DL 2540F membrane element

Sample #	Rejection rate (%)	Pressure (PSI)	Flowrate GPM	Temperature (°C)
1	98.32	50	2	25.7
2	99.54	50	2	30
3	99.03	50	2	35
4	99.37	50	2	40
5	99.96	50	2	45
6	98.95	100	2	25
7	98.99	100	2	30
8	99.96	100	2	35
9	99.79	100	2	40
10	99.66	100	2	45

Table B-5 Chloride passage Test of DL 2540F membrane element

Sample #	Rejection rate (%)	Pressure (PSI)	Flowrate GPM	Temperature (℃)
1	92.51	50	2	25.7
2	86.60	50	2	30
3	98.93	50	2	35
4	98.66	50	2	40
5	87.10	50	2	45
6	99.81	100	2	25
7	98.30	100	2	30
8	93.85	100	2	35
9	91.23	100	2	40
10	92.90	100	2	45

Table B-6 Permeate Flux Test of DL 2540F membrane element

Permeate Volume (ml)	Time (s)	Permeate (ml/s)	Ave Permeate (ml/s)	Temperature (℃)	Pressure (psig)	Flowrate (GPM)
47.7	10.82	4.41				
48.0	10.84	4.43	4.41	30	50	2
45.7	10.37	4.41				
46.7	5.28	8.84				
48.7	5.50	8.85	8.86	30	75	2
48.0	5.40	8.89				
47.7	3.59	13.29				
47.0	3.50	13.43	13.37	30	100	2
48.9	3.65	13.40				
47.8	2.75	17.38				
48.5	2.78	17.45	17.48	30	125	2
49.0	2.78	17.63				
49.8	2.19	22.74				
48.0	2.12	22.64	22.60	30	150	2
49.1	2.19	22.42				
48.0	7.25	6.62				
47.5	7.09	6.70	6.67	45	50	2
47.0	7.03	6.69				
44.5	3.47	12.82				
47.0	3.69	12.74	12.77	45	75	2
47.0	3.69	12.74				
47.5	2.47	19.23				
48.2	2.50	19.28	19.27	45	100	2
48.8	2.53	19.29				
44.0	1.69	26.04				
46.2	1.84	25.11	25.47	45	125	2
48.0	1.90	25.26				
42.5	1.32	32.20				
48.8	1.60	30.50	31.11	45	150	2
49.0	1.60	30.63				

Appendix C – TriSep XN45-2540 Nanofiltration Membrane Test

Date: April 27, 2004

Membrane Type: TriSep XN45-2540 Nanofiltration Membrane Element

Pressure: 50 psig Feed Flowrate: 2 GPM

Sodium sulfate concentration in feed: 7.78 g/l

Sodium chloride concentration in feed: 178.04 g/l

Table C-1 Sulfate Rejection Test of XN45-2540 membrane element

Sample #	Sulfate Rejection (%)	Pressure (psig)	Feed flowrate (GMP)	Temperature (°C)
1	85.23	50	2	20
2	82.60	50	2	25
3	79.72	50	2	30
4	77.24	50	2	35
5	75.01	50	2	40
6	72.75	50	2	45
7	95.05	100	2	20
8	94.57	100	2	25
9	93.75	100	2	30
10	92.45	100	2	35
11	91.16	100	2	40
12	89.53	100	2	45

Table C-2 Chloride Passage Test of XN 45-2540 membrane element

Sample #	Chloride Passage (%)	Pressure (psig)	Feed flowrate (GMP)	Temperature (°C)
1	70.75	50	2	20
2	70.43	50	2	25
3	66.79	50	2	30
4	61.09	50	2	35
5	58.87	50	2	40
6	58.66	50	2	45
7	58.98	100	2	20
8	63.41	100	2	25
9	66.95	100	2	30
10	63.67	100	2	35
11	62.57	100	2	40
12	63.31	100	2	45

Table C-3 Permeate Flux Test of XN 45-2540 membrane element

Sample #	Permeate Volume (ml)	Time (s)	Permeate (ml/s)	Temperature (°C)	Pressure (psig)	Flowrate (GPM)
1	49.60	24.94	1.99	20	50	2
2	47.50	20.20	2.35	25	50	2
3	47.20	17.00	2.78	30	50	2
4	46.80	14.50	3.23	35	50	2
5	48.20	12.87	3.75	40	50	2
6	48.80	11.29	4.32	45	50	2
7	46.50	9.75	4.77	20	100	2
8	48.70	8.60	5.66	25	100	2
9	48.50	7.25	6.69	30	100	2
10	46.80	5.97	7.84	35	100	2
11	47.20	5.09	9.27	40	100	2
12	48.00	4.34	11.06	45	100	2

Appendix D – FilmTec NF270-2540 Nanofiltration Membrane Volume Reduction Test

Date: May 27, 2004

Membrane Type: FilmTec (DOW) NF270-2540 Nanofiltration Membrane Element

Pressure: 150 psig Temperature: 45°C Feed Flowrate: 5 GPM

First Batch

Initial sodium sulfate concentration in feed: 9.35 g/l

Initial sodium chloride concentration in feed: 197.35 g/l

Table D-1 Sulfate Rejection Test of NF270-2540 membrane element

# of run	Sulfate concentration in permeate (g/l)	Sulfate concentration in feed (g/l)	Sulfate Rejection (%)
1	0.02	9.72	99.81
2	0.01	9.96	99.86
3	0.09	11.59	99.23
4	0.11	14.41	99.26
5	0.10	16.19	99.38
6	0.05	18.12	99.71
7	0.17	20.56	99.18
8	0.39	23.46	98.33
9	0.52	25.73	97.99

Table D-2 Chloride Passage Test of NF270-2540 membrane element

# of run	Chloride concentration in permeate (g/l)	Chloride concentration in feed (g/l)	Chloride Passage (%)
1	197.35	189.81	98.52
2	194.43	199.50	89.36
3	176.36	183.97	91.44
4	180.45	176.63	82.43
5	162.68	198.14	92.70
6	182.94	186.99	93.08
7	183.69	190.22	82.14
8	162.11	195.98	86.33
9	170.38	193.68	85.93

Table D-3 Permeate Flux Test of NF270-2540 membrane element

# of run	Feed Flowrate (GPM)	P1-P2 (PSI)	Permeate volume (ml)	Time (s)	Permeate (ml/l)	Flux (GPM)
	1.27	1.0	44.90	2.62	17.14	0.27
	2.30	2.5	50.00	2.63	19.01	0.30
1	3.30	4.0	50.00	2.63	19.01	0.30
	4.28	5.5	44.80	2.50	17.92	0.28
	5.27	7.0	45.00	2.63	17.11	0.27
	1.26	1.0	47.5	2.81	16.90	0.26
	2.28	2.0	48.5	2.68	18.10	0.28
2	3.28	3.5	48.7	2.72	17.90	0.28
	4.29	5.0	49.5	2.66	18.61	0.29
	5.27	7.0	44.8	2.63	17.03	0.27
	1.24	0.5	48.8	3.12	15.64	0.24
	2.26	2.0	46.8	2.81	16.65	0.26
3	3.27	3.0	47	2.75	17.09	0.27
	4.26	5.0	47	2.87	16.38	0.26
	5.25	7.0	47.5	3	15.83	0.25
	1.24	1.0	47.5	3.13	15.18	0.24
	2.25	2.5	48.7	3.09	15.76	0.25
4	3.25	4.0	47.8	3.03	15.78	0.25
	4.25	5.0	49	3.03	16.17	0.25
	5.25	7.0	47	2.97	15.82	0.25
	1.21	1.0	48.5	3.57	13.59	0.21
	2.23	2.0	47.5	3.28	14.48	0.23
5	3.23	3.0	49	3.32	14.76	0.23
	4.24	4.0	49.6	3.28	15.12	0.24
	5.23	7.0	48.8	3.28	14.88	0.23
	1.20	1.0	49.5	3.87	12.79	0.20
	2.21	2.0	48.5	3.53	13.74	0.21
6	3.21	3.0	48	3.5	13.71	0.21
	4.21	4.5	49	3.65	13.42	0.21
	5.22	7.0	49	3.54	13.84	0.22
	1.18	1.0	48	4.25	11.29	0.18
	2.19	2.0	46.8	3.87	12.09	0.19
7	3.19	4.0	46	3.78	12.17	0.19
	4.19	5.0	47.6	3.91	12.17	0.19
	5.19	7.0	46	3.75	12.27	0.19
	1.16	1.0	47.6	4.78	9.96	0.16
	2.17	2.0	47.8	4.47	10.69	0.17
8	3.17	4.0	48.3	4.5	10.73	0.17
	4.17	5.0	48	4.41	10.88	0.17
	5.16	7.0	46.8	4.47	10.47	0.16
	1.13	0.5	47	5.5	8.55	0.13
	2.14	2.0	46.5	5.19	8.96	0.14
9	3.15	3.0	48.5	5.21	9.31	0.15
	4.15	5.0	49	5.13	9.55	0.15
	5.15	7.0	47.5	5.03	9.44	0.15
	1.11	1.0	45.6	6.5	7.02	0.11
	2.12	2.0	48	6.5	7.38	0.12
10	3.12	3.0	46.7	6.16	7.58	0.12
	4.12	5.0	47.8	6.25	7.65	0.12
	5.12	7.0	47.9	6.31	7.59	0.12

Date: June 15, 2004

Membrane Type: FilmTec (DOW) NF270-2540 Nanofiltration Membrane Element

Pressure: 150 psig Temperature: 45°C Feed Flowrate: 5 GPM

Second Batch

Initial sodium sulfate concentration in feed: 25.31 g/l

Initial sodium chloride concentration in feed: 189.81 g/l

Table D-4 Sulfate Rejection Test of NF270-2540 membrane element

# of run #	Sulfate concentration in permeate (g/l)	Sulfate concentration in feed (g/l)	Sulfate Rejection (%)
1	3.06	29.60	89.65
2	4.06	33.13	87.75
3	6.81	37.69	81.93
4	8.87	41.40	78.57
5	14.18	46.77	69.68
6	14.64	51.70	71.68
7	16.05	54.08	70.33
8	24.11	56.51	57.33

Table D-5 Permeate Flux Test of NF270-2540 membrane element

# of run	Feed Flowrate (GPM)	Pressure drop P1-P2 (PSI)	Permeate Volume (ml)	Permeate Time (s)	Permeate ml/l	Permeate Flux (GPM)
1	1.13	1.0	48.9	5.75	8.50	0.13
	2.14	3.0	48.5	5.38	9.01	0.14
	3.14	5.0	49.3	5.41	9.11	0.14
	4.15	9.0	49.7	5.25	9.47	0.15
	5.15	11.0	49.5	5.32	9.30	0.15
2	1.11	1.0	47.6	6.72	7.08	0.11
	2.12	3.0	47	6.37	7.38	0.12
	3.12	4.0	49.2	6.59	7.47	0.12
	4.12	6.0	48.7	6.38	7.63	0.12
	5.12	11.0	48.6	6.5	7.48	0.12
3	1.09	1.0	48.1	8.41	5.72	0.09
	2.09	3.0	48.5	8.13	5.97	0.09
	3.10	4.0	49.5	8.07	6.13	0.10
	4.10	6.0	46.4	7.56	6.14	0.10
	5.10	11.0	49.5	7.97	6.21	0.10
4	1.07	1.0	48.5	11.31	4.29	0.07
	2.07	3.0	48.6	10.91	4.45	0.07
	3.07	4.0	49.5	10.87	4.55	0.07
	4.07	5.0	48.5	10.53	4.61	0.07
	5.07	11.0	49.5	11	4.50	0.07
5	1.05	1.0	48.5	15.66	3.10	0.05
	2.05	2.0	49.3	15.15	3.25	0.05
	3.05	4.0	49.7	15.44	3.22	0.05
	4.05	5.0	48.2	14.84	3.25	0.05
	5.05	11.0	49.5	15.25	3.25	0.05
6	1.03	1.0	48.1	23.44	2.05	0.03
	2.03	2.0	48.5	23.34	2.08	0.03
	3.03	3.0	48.9	23.59	2.07	0.03
	4.03	5.0	49	24.44	2.00	0.03
	5.03	7.0	49.2	23.97	2.05	0.03
7	1.02	0.5	48.5	36.66	1.32	0.02
	2.02	2.0	49	37.72	1.30	0.02
	3.02	3.0	48.8	37.28	1.31	0.02
	4.02	5.0	48.1	38.37	1.25	0.02
	5.02	11.0	49	41.22	1.19	0.02
8	1.01	1.0	48.2	53.87	0.89	0.01
	2.01	2.0	48	53.53	0.90	0.01
	3.01	3.0	49.3	54.72	0.90	0.01
	4.01	5.0	49.2	57.35	0.86	0.01
	5.01	11.0	48.5	59.5	0.82	0.01

Appendix E – GE DL2540F Nanofiltration Membrane Volume Reduction Test

Date: June 1, 2004

Membrane Type: GE DL2540F Nanofiltration Membrane Element

Pressure: 150 psig Temperature: 45°C Feed Flowrate: 5 GPM

First Batch

Initial sodium sulfate concentration in feed: 9.55 g/l

Initial sodium chloride concentration in feed: 204.92 g/l

Table E-1 Sulfate Rejection Test of DL2540F membrane element

# of run	Sulfate concentration in permeate (g/l)	Sulfate concentration in feed (g/l)	Sulfate Rejection (%)
1	0.39	9.97	96.06
2	0.34	11.54	97.05
3	0.78	13.20	94.09
4	0.88	14.99	94.15
5	1.08	17.82	93.93
6	1.31	22.24	94.11
7	1.73	23.12	92.50
8	2.19	26.17	91.63
9	2.42	29.14	91.70

Table E-2 Chloride Passage Test of DL2540F membrane element

# of run	Chloride concentration in permeate (g/l)	Chloride concentration in feed (g/l)	Chloride Passage (%)
1	183.58	188.94	97.16
2	191.76	186.78	99.00
3	199.19	175.40	99.00
4	175.40	189.22	92.70
5	191.20	171.93	99.00
6	194.86	190.35	99.00
7	193.73	187.44	99.50
8	197.59	188.38	99.50
9	187.81	184.99	99.00

Table E-3 Permeate Flux Test of DL2540F membrane element

# of run	Feed Flowrate (GPM)	Pressure drop P1-P2 (PSI)	Permeate Volume (ml)	Permeate Time (s)	Permeate ml/s	Flux (GPM)
	1.41	2	199	7.66	25.98	0.41
	2.43	3	226	8.13	27.80	0.43
1	3.43	5	215	7.72	27.85	0.43
	4.43	8	209	7.47	27.98	0.43
	5.43	11	219	7.94	27.58	0.43
	1.38	2	221	9.1	24.29	0.38
	2.40	3	201	7.75	25.94	0.40
2	3.41	4	198	7.47	26.51	0.41
	4.41	8	215	8.19	26.25	0.41
	5.40	11	205	7.91	25.92	0.40
	1.32	1.5	224	10.9	20.55	0.32
	2.37	3	208	8.72	23.85	0.37
3	3.38	4	210	8.62	24.36	0.38
	4.38	8	222	9	24.67	0.38
	5.39	11	202	8.03	25.16	0.39
	1.18	1.5	47.1	4.06	11.60	0.18
	2.19	3	45	3.72	12.10	0.19
4	3.19	4	44.8	3.66	12.24	0.19
	4.19	8	47	3.81	12.34	0.19
	5.19	11	48.5	4	12.13	0.19
	1.16	2	45.1	4.53	9.96	0.16
	2.17	3	46	4.32	10.65	0.17
5	3.17	5	48.2	4.31	11.18	0.17
	4.17	8	46.5	4.22	11.02	0.17
	5.17	11	47	4.44	10.59	0.17
	1.13	2	46	5.34	8.61	0.13
	2.15	3	47.2	4.97	9.50	0.15
6	3.15	5	48.3	5.13	9.42	0.15
	4.15	7	46.8	5	9.36	0.15
	5.14	11	48.5	5.37	9.03	0.14
	1.11	2	44.6	6.13	7.28	0.11
	2.12	3	47	6.03	7.79	0.12
7	3.12	5	46.2	5.91	7.82	0.12
	4.13	7	48	5.93	8.09	0.13
	5.12	11	48.5	6.41	7.57	0.12
	1.09	1	46.8	8.13	5.76	0.09
	2.10	3	48.8	7.53	6.48	0.10
8	3.10	5	48.4	7.28	6.65	0.10
	4.10	7	47.5	7.41	6.41	0.10
	5.10	11	48.5	7.66	6.33	0.10
	1.07	1	46	9.69	4.75	0.07
	2.08	3	44.7	8.69	5.14	0.08
9	3.08	5	45.7	9.09	5.03	0.08
	4.08	7	46.8	9.03	5.18	0.08
	5.08	11	48	9.88	4.86	0.08

Date: June 7, 2004

Membrane Type: GE DL2540F Nanofiltration Membrane Element

Pressure: 150 psig Temperature: 45°C Feed Flowrate: 5 GPM

Second Batch

Initial sodium sulfate concentration in feed: 24.18 g/l

Initial sodium chloride concentration in feed: 217.14 g/l

Table E-4 Sulfate Rejection Test of DL2540F membrane element

# of run	Sulfate concentration in permeate (g/l)	Sulfate concentration in feed (g/l)	Sulfate Rejection (%)
1	3.12	24.18	87.11
2	3.78	25.90	85.41
3	5.31	28.86	81.60
4	6.14	31.93	80.78
5	3.67	36.22	89.88
6	6.03	39.86	84.88

Table E-5 Chloride Passage Test of DL2540F membrane element

# of run	Chloride concentration in permeate (g/l)	Chloride concentration in feed (g/l)	Chloride Passage (%)
1	191.10	217.14	88.01
2	174.46	207.74	83.98
3	179.73	221.28	81.22
4	179.45	215.17	83.40
5	197.40	210.09	93.96
6	173.71	197.40	88.00

Table E-6 Permeate Flux Test of DL2540F membrane element

# of run	Feed Flowrate (GPM)	Pressure drop P1-P2 (PSI)	Permeate Volume (ml)	Permeate Time (s)	Permeate ml/s	Permeate Flux (GPM)
	1.07	2	49	10.88	4.50	0.07
	2.08	3	48.5	9.69	5.01	0.08
1	3.08	4	47.8	9.4	5.09	0.08
	4.08	7	49.6	10.15	4.89	0.08
	5.08	10	47.5	9.69	4.90	0.08
	1.05	2	48.5	15.5	3.13	0.05
	2.05	3	48	14.03	3.42	0.05
2	3.06	4	48	13.21	3.63	0.06
	4.05	7	49.4	14.5	3.41	0.05
	5.05	10	48	14.88	3.23	0.05
	1.04	2	47.7	19.69	2.42	0.04
	2.04	3	47.9	19.81	2.42	0.04
3	3.04	4	48	20.81	2.31	0.04
	4.04	7	48.5	20.34	2.38	0.04
	5.03	10	48.8	22.22	2.20	0.03
	1.03	1	47.7	25.68	1.86	0.03
	2.03	3	48.5	25.6	1.89	0.03
4	3.03	5	48.7	25.87	1.88	0.03
	4.03	7	48.5	26.15	1.85	0.03
	5.03	11	48.5	28.56	1.70	0.03
	1.03	1	47.7	25.68	1.86	0.03
	2.03	3	48.5	25.6	1.89	0.03
5	3.03	5	48.7	25.87	1.88	0.03
	4.03	7	48.5	26.15	1.85	0.03
	5.03	11	48.5	28.56	1.70	0.03
	1.07	1	47.9	10.07	4.76	0.07
	2.08	3	47.2	8.85	5.33	0.08
6	3.09	5	49	8.91	5.50	0.09
	4.09	7	48.9	8.68	5.63	0.09
	5.08	10	48.2	8.87	5.43	0.08

Appendix F – Distilled Water Permeability Test for GE DL2540F Nanofiltration

Date: April 26 2004

Table F-1 Distilled Water Permeate Flux for DL2540F Membrane

Temperature °C	Pressure (psig)		Flowrate (GPM)	Permeate			Average Permeate (ml/s)	Average Permeate GPM
	P1	P2		Volume (ml)	Time (s)	ml/s		
29	150	140	4	475	6.59	72.08	71.71	1.14
				478	6.70	71.34		
	150	148	1	478	6.47	73.88	73.83	1.17
				484	6.56	73.78		
29.5	100	91	4	483	10.09	47.87	47.92	0.76
				495	10.32	47.97		
29.8	100	98	1	483	9.40	51.38	51.28	0.81
				496	9.69	51.19		
30.4	50	40	4	490	22.25	22.02	22.15	0.35
				484	21.72	22.28		
30	50	48	1	486	20.10	24.18	24.28	0.38
				474	19.44	24.38		

P1: pressure reading at the beginning of membrane housing

P2: pressure reading at the end of membrane housing

Date: April 19 2004

Table F-2 Distilled Water Permeate Flux for DL2540F Membrane

Temperature °C	Pressure (psig)		Flowmeter (GPM)	Permeate			Average Permeate (ml/s)	Average Permeate GPM
	P1	P2		Volume (ml)	Time (s)	ml/s		
19.5	50	53	2	214	10.85	19.72	19.91	0.32
				213	10.75	19.81		
				217	10.82	20.06		
				215	10.72	20.06		
20.4	75	72.6	2	228	7.41	30.77	30.93	0.49
				214	6.93	30.88		
				223	7.16	31.15		
20.3	100	98	2	232	5.32	43.61	43.91	0.70
				233	5.06	46.05		
				221	5.13	43.08		
				224	5.22	42.91		
21	125	123	2	235	4.22	55.69	55.16	0.87
				226	4.15	54.46		
				228	4.12	55.34		
21.4	150	148	2	212	3.19	66.46	67.98	1.08
				220	3.22	68.32		
				231	3.34	69.16		

P1: pressure reading at the beginning of membrane housing

P2: pressure reading at the end of membrane housing

Date: April 28 2005

Table F-3 Distilled Water Permeate Flux for DL2540F Membrane

Temperature °C	Pressure (psig)		Flowrate (GPM)	Permeate			Average	Average Permeate (GPM)
	P1	P2		Volume (ml)	Time (s)	ml/s	Permeate (ml/s)	GPM
19	50	45	2	482	26.69	18.06	18.15	0.29
				492	26.97	18.24		
19.7	75	70	2	494	17.35	28.47	28.63	0.45
				474	16.47	28.78		
20	100	95	2	484	12.35	39.19	38.87	0.62
				487	12.63	38.56		
20	125	121	2	490	10.07	48.66	48.70	0.77
				483	9.91	48.74		
19.9	150	145	2	494	8.38	58.95	58.93	0.93
				486	8.25	58.91		
20	175	170	2	494	7.12	69.38	68.99	1.09
				483	7.04	68.61		
20	200	196	2	471	6.07	77.59	78.20	1.24
				497	6.32	78.64		
				478	6.10	78.36		

P1: pressure reading at the beginning of membrane housing

P2: pressure reading at the end of membrane housing